DEVELOPMENT OF π-CONJUGATED POLYMER SENSORS AND ORGANIC PHOSPHORS FOR LUMINESCENT MATERIALS

Thesis Submitted towards the Partial fulfillment of
BS-MS dual degree programme

IISER PUNE

By

VIKASH KUMAR

20091003

Department of Chemistry

Indian Institute of Science Education and Research (IISER)

Dr. Homi Bhabha Road, Pune 411008

Maharashtra, India

April 2014

Dr. M. Jayakannan

Associate Professor
Department of Chemistry

CERTIFICATE

This is to certify that this dissertation entitled "**DEVELOPMENT OF π-CONJUGATED POLYMER SENSORS AND ORGANIC PHOSPHORS FOR LUMINESCENT MATERIALS**" towards the partial fulfillment of the BS-MS dual degree programme at Indian Institute of Science Education and Research, Pune represents original research carried out by Vikash Kumar, IISER, Pune under my supervision at IISER, Pune during the academic year 2013-2014.

Date:

Place: Signature

DECLARATION

I hereby declare that the matter embodied in the report entitled "**DEVELOPMENT OF π-CONJUGATED POLYMER SENSORS AND ORGANIC PHOSPHORS FOR LUMINESCENT MATERIALS"** are the results of the investigations carried out by me at the Department of Chemistry, IISER Pune, under the supervision of Dr. M. Jayakannan and the same has not been submitted elsewhere for any other degree.

Date:

Place: Signature

ACKNOWLEDGEMENT

CONTENTS   Page

1. ABSTRACT

The problem addressed in this thesis is the study of a π conjugated polymer bearing distilbene unit and functionalized with carboxylic acid for detecting multiple species i.e temperature, Cu^{2+} ions and amino acids by three independent processes (i) red fluorescent temperature switch via ligand to metal energy transfer (LMET) from the polymer to Eu^{3+} ions, (ii) blue fluorescent metal-ion switch by heavy atom effect and exclusive selectivity for Cu^{2+} ions and (iii) as biomolecule switch for the amino acids. Because of the presence of coligand these are difficult to process into device and to take care of this, five different ligands are designed rationally bearing Iodine as heavy atom substituted strategically on the chromophore unit that can sensitize europium metal ion even in absence of a coligand through singlet to triplet state intersystem crossing. These ligands are characterized by 1H NMR, 13C NMR and MALDI analysis and their photophysical properties are studied in solution and solid state to see if they are phosphorescent or not. These were also studied using time resolved luminescent decay profiles to see the lifetime of species emitting at respective wavelengths. Effect of packing leading to triplet state population generation/phosphorescence was studied using DSC analysis and emission studies of annealed samples. These ligands were then complexed with Europium metal ion and were characterized using IR and MALDI-TOF. The complexes showed bright red emission under UV light and their emission spectra showed five sharp peaks corresponding to D-F transitions confirming the fact that these ligands sensitize europium metal ion through enhancement of population in triplet level without any involvement of a coligand.

2. INTRODUCTION

2.1 Lanthanide complexes: New classes of luminescent materials.

In the periodic table, trivalent lanthanide ions are well arranged from La to Lu based on their electronic configurations $[Xe]4f^n$ and the gradual filling of the 4f orbitals, from $4f^0$ (for La^{3+}) to $4f^{14}$ (for Lu^{3+}). These special features provide interesting emission properties for lanthanide metal ions[1] (Binnemans, K. 2009) as shown in figure 2.1. Emission colors purely depend on individual lanthanide ion. Upon irradiation of ultra violet radiation, some of the metal ions are emitting in the visible region or near infra red region. For example, red, green, orange and blue color emissions arise from Eu^{3+}, Tb^{3+}, Sm^{3+}, and Tm^{3+} metal ions, respectively. Yb^{3+}, Nd^{3+}, and Er^{3+} metal ions are well-known for producing emission at near infra red region and remaining lanthanide metal ions (Pr^{3+}, Sm^{3+}, Dy^{3+}, Ho^{3+}, and Tm^{3+}) also have some transition in the Near IR region[2] (in figure 2.1) (Bunzli. 2010). The luminescence of lanthanides arises due to intraconfigurational f-f transitions of 4f orbitals which are parity and spin forbidden. The partially filled f orbitals are well shielded from outside environment by closed $5s^2$ and $5p^6$
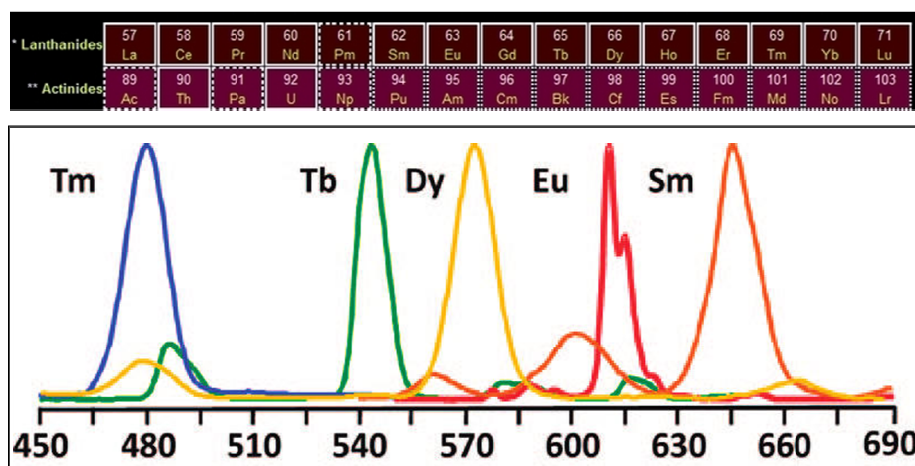
Fig 2.1 Emission profiles of various Ln^{3+} metal ions

sub-shells and also the electronic configuration of trivalent lanthanides is perturbed to very limited extent by first and second coordination sphere of the ligands[2] (Bunzli. 2010). This shielding effect as well as the parity forbidden nature of the f-f transitions is responsible for the unique photophysical properties of lanthanide ions more specifically for narrow band (sharp) emission and long excited state lifetime. The excited state lifetime of the lanthanide ions are in the range of 10^{-6} seconds to 10^{-3} seconds. But

although the lanthanides have long lifetime and unique emission feature, they are very weakly absorbing because of their low molar absorption coefficients. This drawback regarding the emission of lanthanides can be overcome by using organic ligands as antenna which have high absorption coefficient. Upon photoexcitation, organic ligands absorb the given radiation, transferring that energy to the lanthanides which then undergo their respective f-f transition leading to very bright emission. This process of photosensitizing lanthanides is called "the antenna effect". This process is very similar to dipole-dipole or Forster energy transfer processes where ligands take part in photosensitization process through excited singlet state and triplet state. Subsequently, the sharp metal centered emissions occurrs followed by emission of lanthanide metal ions to ground state through intraconfigurational f-f transitions[3]. In 1997, Latva and coworkers had reported library of coordinating ligands containing various range of triplet energy levels and correlated with quantum efficiency of lanthanide complexes. Based on the quantum efficiency and triplet state energy levels, they postulated an empirical rule for efficient energy transfer from triplet state of ligands
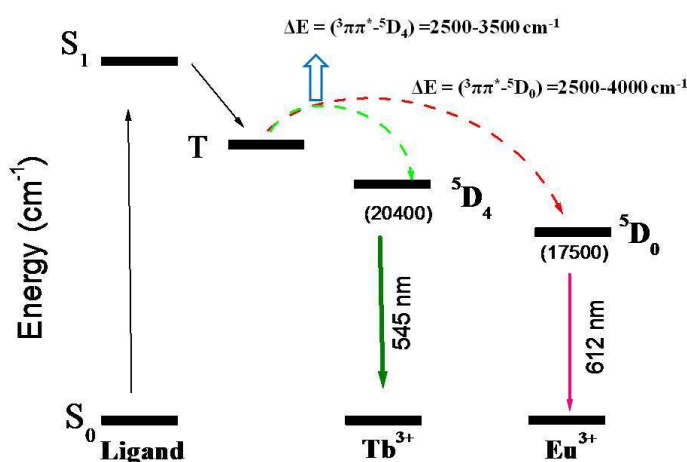
Fig 2.2 Schematic diagram of Latva's empirical diagram for energy transfer process for Ln^{3+} ions.

to excited state of the metal center and this rule is called Latva's empirical rule (Latva, M. et al. 1997). It states that an optimal ligand-to-metal energy transfer process for Eu^{3+} requires ΔE ($^3\pi\pi^*$-$^5D_0$) = 2500-4000 cm^{-1} and for Tb^{3+} ΔE ($^3\pi\pi$-$^5D_4$) = 2500-4500 cm^{-1}. It was well recognized and accepted rule for energy transfer process in most of the organic ligand-lanthanide complexes (figure 2.2).

2.2 Polymer lanthanide hybrid systems

A shift from small molecules to the polymeric system has started taking place as they possess unique physical and optical properties of both polymers and lanthanide complexes. In that regard, aromatic π-conjugated polymer-lanthanide hybrid materials are emerging as important class of candidates for the application in the field of opto-electronics. These hybrid materials possess unique features of both polymers and lanthanide complexes; for example mechanical and thermal stability, flexibility, film forming tendency of polymers along with unique optical properties of the lanthanides. New classes of functionalized π-conjugated polymers based on carboxylic functionalized poly(m-phenylenevinylene)s and poly(m-phenylene)s are custom designed and utilized as potential photosensitizer for producing new polymer-lanthanide hybrid luminescent materials[4]. Further, efforts have been put to trace the photosensing mechanism via detailed photophysical studies such as emission, excitation and time resolved luminescent decay dynamics. Apart from this, the polymer chain aggregation induced nano-particles photoemission in water and temperature dependent sensing of the polymer-lanthanide complexes have also been achieved. Extensive research in this field has been done by Balamurugan et al[4]. They have demonstrated a facile molecular approach to generate white light emission by combining carboxylic functionalized poly(m-phenylenevinylene)s polymeric architectures with lanthanide β-diketonate complexes. The new class of carboxylic functional conjugated polymeric materials was custom-designed from phenyl propionic and acetic acid. These designed conjugated polymers were employed for the synthesis of lanthanide complexes in the presence of acetyl acetone (acac) as co-ligand and their photophysical properties was investigated[4]. Investigations revealed that carboxylic functionalized polymeric material with Eu^{3+}-β-diketonate complex exhibited unique magenta emission when excited at 310 nm while Tb^{3+}-β-diketonate complex showed bright sky-blue emission. Interestingly, when Eu^{3+} and Tb^{3+} were incorporated into polymer backbone in equimolar ratio along with acetyl acetone as co-ligand, white light emission was obtained (as shown in figure 2.3).
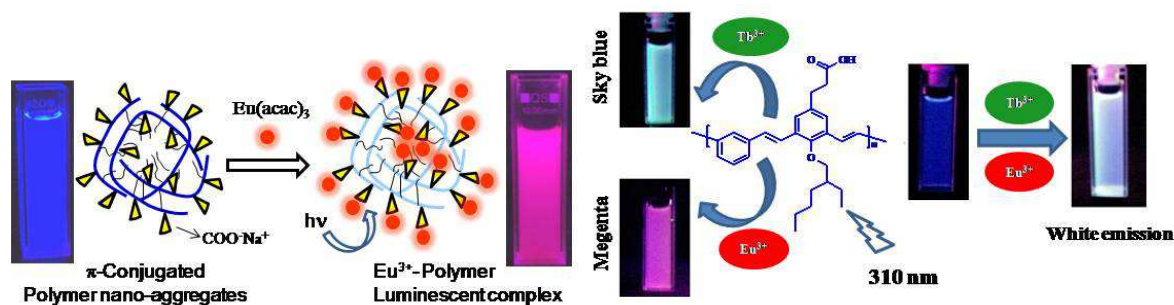
Fig 2.3 Emission behavior of polymer lanthanide complexes

These carboxylic functionalized poly(phenylene)s and their oligomers were synthesized by Palladium catalyzed Suzuki polycondensation. The chemical structures of the polymer skeleton were varied using two anchoring groups consisting of branched-ethylhexyloxy and simple methoxy substitution in the chain backbone. Photoexcitation of the oligomer-Eu^{3+} complexes resulted in the magenta color emission as a result of the combination of partial blue self-emission from the chromophores along with the red-color from the metal center while the ethylhexyl substituted polymer- Eu^{3+} complex showed complete excitation energy transfer from the macromolecular chains to the metal center and produced bright and sharp red emission. The molecular self-organization of the polymers was found to play a crucial role on the efficient energy transfer from the polymer chain to metal centre, more specifically Eu^{3+} ions based red emission[4].

One of the ways to make such polymer lanthanide hybrid system is the post metal complexation of polymers. In this method, the polymers containing coordinating functional group (carboxylic acid, terpyridine and pyridine etc.) are synthesized and post complexed with Ln^{3+} metal ions to achieve mechanically stable polymer-lanthanide hybrid materials. Thermally stable carboxylic functionalized polyaryletherketone[5] (PEK1) developed by Liu and coworkers for coordinating with $Tb^{3+}$and Eu^{3+} ions using phenonthroline[6] (Phen), 8-hydroxyquinoline (HQ) and dibenzoylmethane (DBM) as co-ligands (Liu, D. et al).
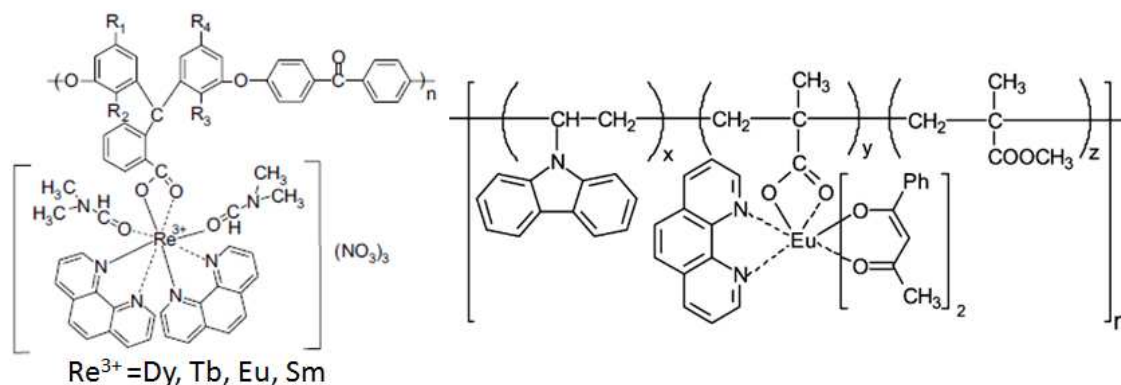
11

Fig 2.4 Post complexation of lanthanide complexes into polymer via covalent linkage.

The use of amphiphilic polymers as coordinating ligand has many advantages in the area of biology and material sciences. The polymeric amphiphiles can self-organize to attain diverse morphologies such as lamellae, vesicles, cylinders, spheres and micelles in the nanometer scale which played vital role in the performance of electronic or optoelectronic applications[7] (Forster, S. et al. 1998) and biological applications like biosensors or immobilization of antibodies[8, 9] etc. (Leonov, A. P. et al. 2008; Ding, H. et al. 2007).

But one great limitation associated with these hybrid polymers is that they need a co-ligand such as diketonic species in addition to the polymeric systems. These co-ligands greatly reduce the sensitivity of the hybrid materials when it comes to bio-sensing or device making because of the poor processibility of hybrid materials which comes as a package with these co-ligands. To counter these problems, modern research on these hybrid systems tend to develop small molecules and polymeric systems which can sensitize lanthanide metal ions without involving any co-ligand. Unfortunately, most of the organic molecules are known to undergo vibration relaxation (as heat) from the excited triplet state to the singlet ground state (via $T \rightarrow S_0$ transition). Though wide range of organic ligands are reported for coordination complexes with lanthanides,[10] still manipulation of triplet state (T) energy levels and channelizing the excitation energy to metal-centre are few of the major problems to be addressed. Hence, optimization of ligand chemical structure as an efficient photosensitizer in absence of coligand for LMET is one of the crucial factors for achieving luminescence in the lanthanides. One such series of ligands was designed by Balamurugan et al where they designed a

series of ligands and their europium based metal organic frameworks (MOFs) by rationally substituting iodine atom on the chromophore unit as shown in figure 2.5
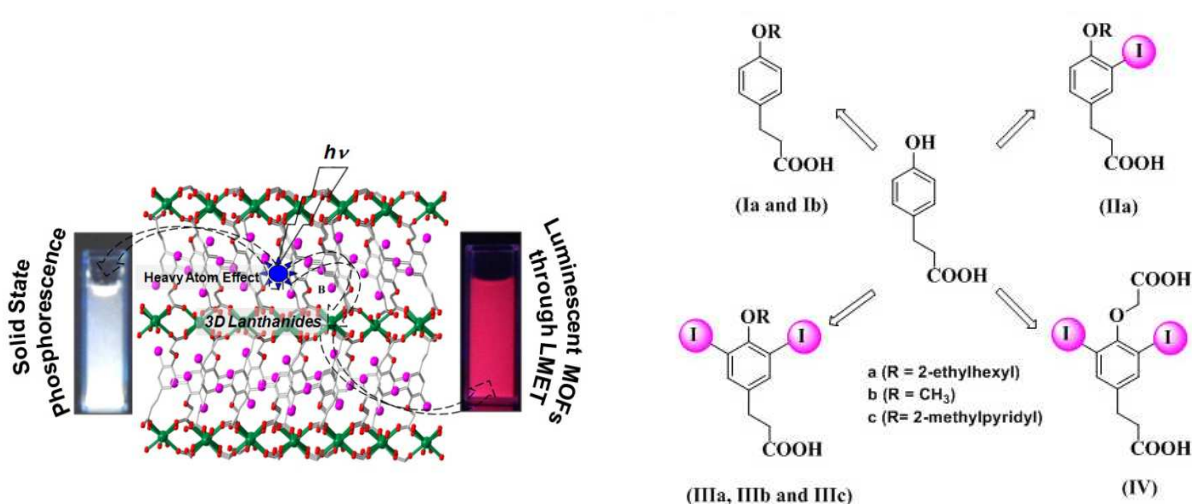
Fig 2.5 Series of engineered ligands for sensitizing Europium by Balamurugan et al

These ligands were called as organic phosphors because they were phosphorescent in absence of lanthanides and upon complexation they effectively transferred their triplet level energy to lanthanides without the help of a coligand.

2.3 Organic phosphors

These are a class of organic compounds that show phosphorescence. When we talk of phosphorescence we usually think of inorganic and organometallic complexes because organic molecules showing phosphorescence are very rare and those which show this property are very weakly phosphorescent which can be easily ignored[11]. Phosphorescent molecules find great application in analyte sensing[12] and light emitting devices such as organic light emitting diodes[13] and the current status of materials developed is that there are plenty of organometallic and inorganic phosphors developed but organic phosphors are seldom reported[14]. But organometallic and inorganic phosphors have their own limitations such as poor processibility, difficult synthesis and solubility. These are the issues which are easily dealt in case of organic phosphors

because of the ease of synthesis and solubility of organic compounds in organic solvents. Organic phosphors are also more important in terms of versatility as we can tune the organic compounds by changing the functionalities to suit it for our need such as generation of different colors owing to the difference in singlet and triplet energy level of organic compounds. So instead of making a number of organometallic or inorganic phosphors we can think of organic molecules whose functionalities can be easily changed leading to the generation of different phosphors without much of   synthetic impedance. One very fundamental question that needs to be addressed is how these organic compounds show phosphorescence. Organometallic complexes and inorganic compounds have heavy metal atoms because of which the spin orbit coupling at the chromophore unit is favored which leads to the generation of excited electrons in the triplet state from the singlet state and it is from the triplet state that they radiatively decay back to the ground state showing phosphorescence[15]. Taking care of the need of heavy atom in organic molecules to design organic phosphors, Bolton et al rationally designed a bromine substituted chromophore that contained carbonyl oxygen[16]. This bromine atom present within the chromophore acted as a heavy atom that interacted with the carbonyl oxygen of other molecule to promote the intersystem crossing of electrons from singlet to triplet state therby showing phosphorescence[17]. This is a landmark discovery for the quest of organic phosphors. Apart from the rational design of organic compounds using heavy atom effect for harvesting triplet emission there are many other parameters that need to be taken care of.   One such parameter is the proximity of heavy atom such as iodine present within the molecule to the chromophore unit of other molecule. The distance between heavy atom and the chromophore unit should be such that they halogen bond with each other[18]. More is the distance then there cannot be effective spin orbit coupling between excited electrons and heavy atom therby limiting the population of electrons in triplet state. Once the distance is within the halogen bonding range then effective spin orbit coupling happens because of which phosphorescence from organic molecules is observed. This observation was observed by Bolton et al where they showed that organic phosphors do not show phosphorescence in solution. In solution each of the organic molecules are far separated from each other because of which there is no halogen bonding but once

these organic molecules are grown into crystals then they show phosphorescence peak in the emission spectra at higher wavelength region as shown in figure 2.6
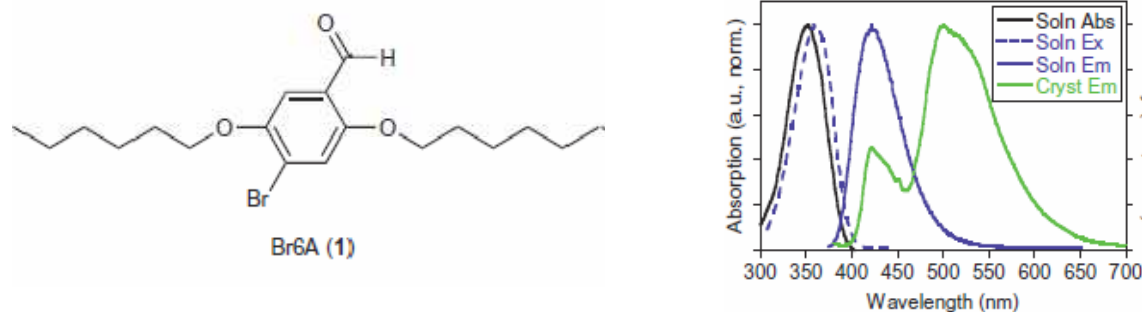

Fig 2.6 Organic phosphor designed by Bolton et al and its emission showing phosphorescence at higher wavelength

This brings into picture the relation of packing of molecules with phosphorescent emission. Better the molecules are packed, better is the alignment of molecules which leads to the fitting of heavy atoms present within the molecule in the bonding range with chromophore unit. Another consideration that needs to be taken care of regarding phosphorescent emission from organic phosphors is the triplet-triplet annihilation[19]. In bulk system although the respective entities responsible for triplet state generation are within the bonding range and triplet states are generated but there is always a possibility of triplet-triplet annihilation leading to the loss of most of the part of triplet radiation as heat. To take care of this drawback Bolton et al doped different concentration of organic phosphors into a matrix therby increasing the phosphorescent emission. One way of quantifying the phosphorescence generated by organic phosphors is by obtaining their quantum yield. The phosphorescence quantum yield of organic phosphors in solution is lowest while in crystalline state, the value of quantum yield is relatively higher.

Upon doping these molecules into a suitable matrix the value of quantum yield increases even more. Same group of Bolton et al doped the organic phosphor as discussed before into PMMA matrix and used it as temperature sensor[20] as shown in figure 2.7
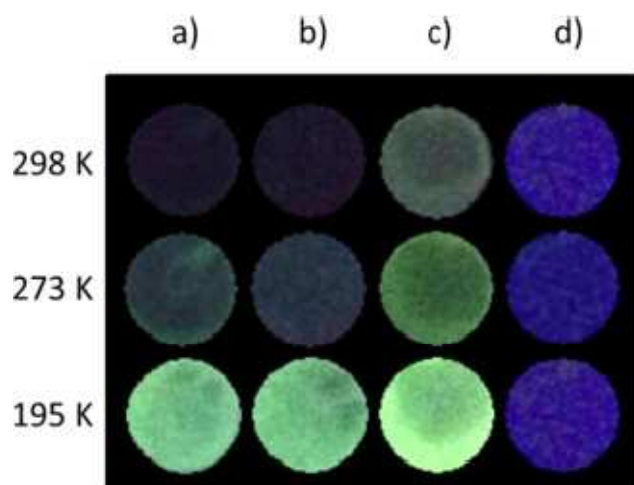
Fig 2.7 Phosphorescence emission of Br6A embedded in (a)atactic PMMA, (b) syndiotactic PMMA, and (c) isotactic PMMA at different temperatures. (d)Blue fluorescence emission of pure Br6A visible in part due to a lack of green phosphorescence also at these temperatures. The excitation wavelength was 365 nm(as reported by Lee et al in JACS)

2.4 Electronic application of organic phosphors

Organic phosphors can be a pivotal player in Organic Light Emitting Diode (OLED) and sensing research because of its long lived radiative triplet emission that is possible even in the absence of coligands.

A major part of energy consumed by electricity is used in lighting applications and in that, significant amount of energy is wasted as heat. Because of this reason there is a dire need of devices that have more efficiency when it comes to power generation by using minimum input. OLEDs are one such class of devices that follow such energy economy[21, 22].

These are multilayered device comprising of metal cathode having high work function, metal oxide anode having low work function, an electron transporting layer, a hole transporting layer and an emissive layer. On connecting cathode and anode using a conducting wire, electrons travel from anode to cathode generating holes at the junction of anode and hole transporting layer. These holes travel through the hole transporting layer and meet the electrons travelling in the electron transporting layer via cathode to

form excitons in the excited state. In the emissive layer, once these excitons relax back to the ground state they emit light corresponding to the energy difference between the ground and excited states[23].
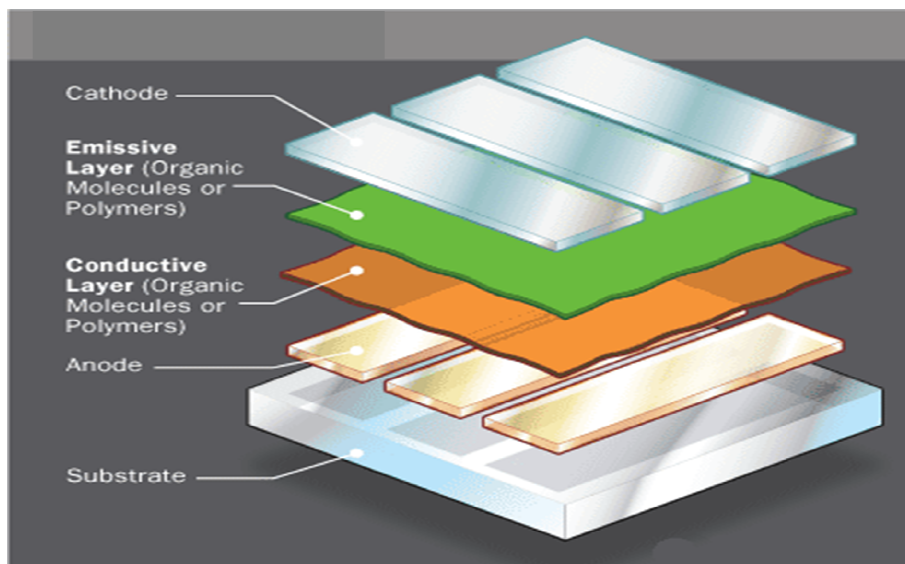
Fig 2.8 Schematic of an organic light emitting diode

Each component of an OLED has its own importance and extensive research is done to make each component more effective and versatile. Emissive layer is one such layer where phosphorescence of molecules is exploited. At the instant when electrons and holes recombine to form excitons there are 4 possibilities of the net spin that is formed because of the individual spin moments of electron and hole[24, 25, 26].

1) one combination of antiparallel spins of electron and hole giving rise to a singlet state of exciton and

2) three combinations of parallel spins of electron and hole giving rise to a triplet state of exciton.

The emissive layer is designed rationally using a polymer backbone as host materials to provide mechanical stability for device integration. This backbone is then doped with singlet and triplet emitters to prevent triplet-triplet annihilation occurring in the host materials present in the emissive layer. The dopants derive their energy from host

17

material and these are designed in such a way that the triplet and singlet energy level of host is higher as compared to the triplet and singlet energy level of the dopant for optimum energy transfer (figure 2.9).
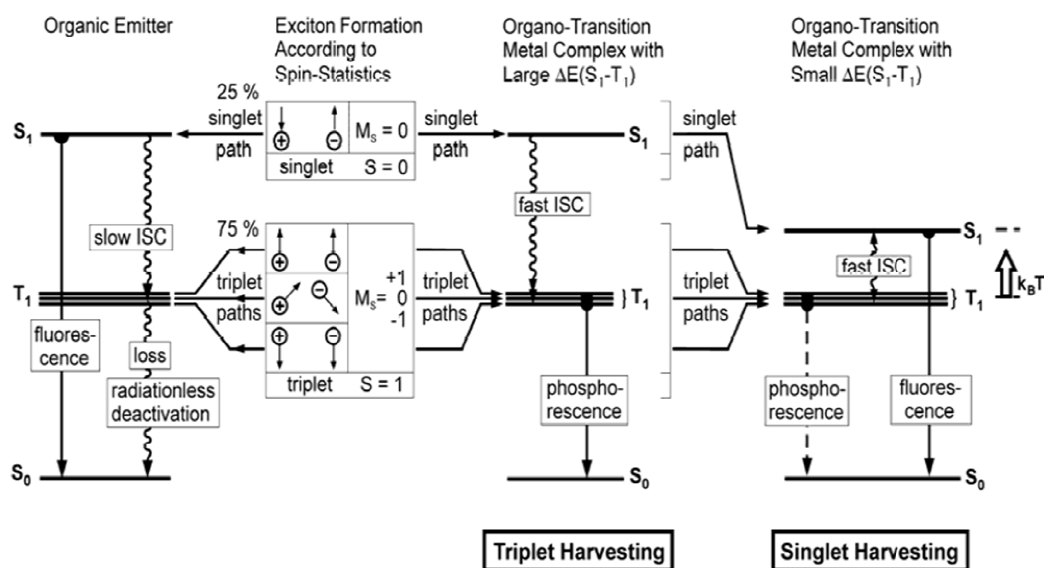

Fig 2.9 Electroluminescence excitation process for organic and organo-transition metal emitters and their singlet and triplet harvesting

If the dopant is only fluorescent in nature then only 25% of the excitons are exploited giving rise to one-fourth external efficiency while if the dopant is phosphorescence that we can exploit 100% excitons realizing 100% external efficiency. But usually triplet energy is wasted as non radiative decay therby limiting the efficiency of organic light emitting diodes. This has led to a thrust in the development of phosphorescent emitters and in the current research scenario organometallic complexes are vital candidate for the same. These organometallic compounds derive their phosphorescence because of the heavy metal atom (such as iridium) that induces spin orbit coupling because of which there is huge population generation in the triplet state which then undergoes radiative transition giving rise to different colors depending on the energy gap.

But these phosphorescent organometallic emitters have their own limitations. They are not easily processible because of poor solubility and the most important limitation is that

they are not versatile. These shortcomings can be overcome if we rationally design pure organic compounds as triplet emitter in dopants because of the fact that they are easily processible and the myriad of derivatives that can be developed with ease because of the functionalities present in pure organic molecules which rules their physical and chemical properties.

2.5 Aim of the thesis

Considering the fact that there have been numerous fluorescent probes for dual sensing of analytes such as ratiometric detection of different metal ions; different anions or metal-ion along with proteins and sugars but there are no reports of a single molecular probe detecting more than two species, the problem addressed in this thesis deals with the application of π conjugated segmented polymers functionalized with carboxylic acid and polyethylene glycol units as spacer for detecting temperature, metal ion and amino acids as shown in figure 2.10. This is because designing new triple or multiple action molecular probes are important for fundamental understanding as well as developing new tools for sensing more than two analytes. Although the molecular probe was aimed at sensing three analytes, a co-ligand was needed for sensing temperature which hinders the development of such system into device making because of poor processibility. Keeping that limitation in mind, five different ligands (L1, L4, L8, L12, L16) are synthesized rationally on the basis of heavy atom effect so as to generate excess population of excited electrons from singlet to triplet state therby showing phosphorescence. These can be called as organic phosphors and they are then complexed with Europium metal to sensitize it as shown in figure 2.11. This makes the Europium metal show sharp emission lines with high molar extinction coefficient which
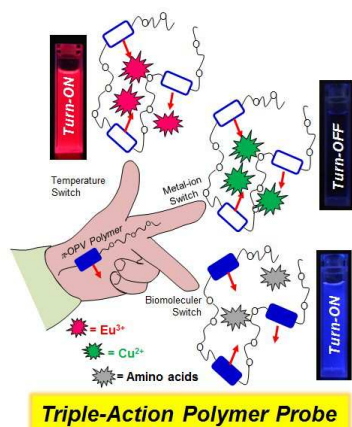
19

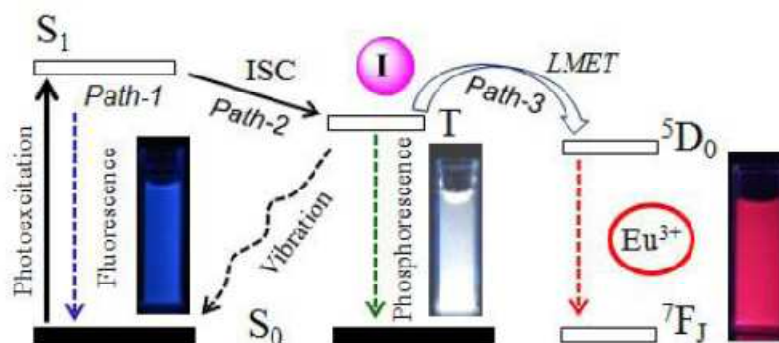*Fig2.10 Triple action polymer*   *Fig2.11 Europium sensitization via triplet state provided by heavy atom*

otherwise is not possible. These organic phosphors and their europium complexes can be a great asset for OLED and biosensing and temperature research because of the easy processibility due to their solubility in organic solvents.

3. MATERIALS AND METHODS

3.1 <u>MATERIALS</u>

3-(4-Hydroxyphenyl)propionic acid, Europium Nitrate pentahydrate and different alkyl bromides were purchased from Sigma Aldrich. Potassium Iodide and Iodine were purchased from RANKEM. Dry solvents such as methanol, acetonitrile and DMSO were purchased from Finar reagents and other solvents such as ethanol was purchased locally. Polymers for sensing studies was designed by Balamurugan et al.

3.2 <u>METHODS</u>

NMR was recorded in 400MHz Jeol NMR spectrometer in $CDCl_3$ for all compounds except 3-(4-Hydroxy-3,5-diiodophenyl)propanoic acid which was done in CD_3OD with TMS as standard. Mass of all the compounds was confirmed using the Applied Biosystems 4800 PLUS MALDI TOF analyzer. FT-IR spectra of all the complexes was recorded on a Thermo Scientific Nicolet 6700 FTIR spectrometer using potassium bromide(KBr) discs prepared from powdered samples mixed with dry KBr. The spectra were recorded in absorbance mode from 4000 to 400 cm^{-1}.Thermal Gravimetric Analysis was performed on a Perkin-Elmer STA 6000 instrument. Absorption and emission studies were performed on a Perkin-Elmer Lambda 45 UV-Visible spectrophotometer and SPEX Fluorolog HORIBA JOBIN VYON fluorescence spectrophotometer with a double grating 0.22m spex 1680 monochromator and a 480W Xe lamp as the excitation source at room temperature. The emission studies of polymers for sensing temperature, metal ion and amino acid was done using 310nm as excitation source while the emission spectra of ligands as well as the complexes was collected using 330nm as the excitation source. The TCSPS decay profile of ligands with respect to fluorescence was collected using 339nm nano-LED laser as excitation source and with respect to phosphorescence was collected using pulsed Tungsten lamp as excitation source. The thermal stability of the ligands was determined using TGA-50 Shimadzu thermogravimetric analyzer at a heating rate of 10 °C/min in N_2 atmosphere. Thermal analysis of the ligands was performed using TA Q20 Differential Scanning Calorimeter. All the ligands were heated to melt before recording their thermograms to remove their previous thermal history. Ligands were heated and cooled at 10 °C/min under N_2 atmosphere and their thermograms were recorded.

3.3 <u>GENERAL PROCEDURES</u>

3.3.1 Temperature sensing studies:

The temperature sensing studies of the polymer-Eu^{3+} complexes were carried out in various solvents tetrahydrofuran, chlorobenzene dimethyl sulfoxide and xylene. The concentration of the polymer-Eu^{3+} complexes were fixed at 1.8×10^{-6} M (0.1OD absorbance) and emission spectra of the complexes were recorded by exciting at 350 nm with various temperatures from 20- 100 °C.

3.3.2 Metal ion sensing studies:
The sensing studies were carried out in 3 mL cuvette and 5μL of polymer solutions (stock solution = 3.2×10^{-3} M) were diluted in the buffer solution. The stock solution of metal perchlorate salts were prepared with 2×10^{-2} M concentrations. The absorbance and fluorescence titration was carried out by adding of 3μM metal solutions into the polymer + PIPES buffer solutions.

3.3.3 Anion sensing studies:

The completely quenched Cu^{2+} bound polymer solutions were prepared by adding the mixture of polymer solutions with 24 μM concentration of Cu^{2+} ions in PIPES buffer soltuions at pH =7.4. The stock solutions of all the amino acids and phosphate ion were prepared with 2×10^{-2} M concentrations. The fluorescence turn on experiment was carried out by successive additions of amino acids to Cu^{2+} bound polymers solutions. The fluorescence spectra of the polymers were recorded for each concentration of amino acid by exciting at 305 nm.

3.3.4 Synthesis of organic phosphors:

3.3.4.1 Synthesis of 3-(4-Hydroxy-3, 5-diiodophenyl)propanoic acid(1)

3-(Hydroxyphenyl)propanoic acid (10.0 g, 60.2mmol) was dissolved in 20% methylamine (100 mL) and stirred at room for about 15 min. KI (28.8 g, 173.6 mmol) and iodine(30.4 g, 120.3 mmol) in water (60 mL) were slowly added into the solution. The solution was stirred for 5 h and after that the mixture was neutralized with 2 N concentrated HCl (100 mL). White precipitate was formed which was filtered and washed with water until the filtrate became neutral. The white solid was further purified

by recrystallization from hot ethanol to obtain needle-like crystals as a product. Yield = 23.0 g (91%). 1H NMR (400 MHz, CD$_3$OD) δ: 7.34 (s, 2H, Ar_H), 2.73 (t, 2H, Ar_CH$_2$CH$_2$), 2.51 (t, 2H,CH$_2$_CH$_2$COOCH$_3$). 13C NMR (100 MHz, CD$_3$OD) δ: 178.92, 157.74, 143.12 (4C), 87.99, 39.16, and 32.52 ppm. MALDI-TOF: MW = 417.97 and m/z = 440.983 (M$^+$ + K$^+$).

3.3.4.2 Synthesis of Methyl-3-(4-hydroxy-3,5-diiodophenyl)propanoate(2)

1(10.0 g, 120.0 mmol) was dissolved in dry methanol (50 mL) in 100 mL RB flask. Concentrated H$_2$SO$_4$ (6 mL) was slowly added into the methanol solution while stirring, and the mixture was refluxed for 12 h after which it was concentrated and poured into water, and the precipitate was filtered and washed with water until the filtrate became neutral. Solid product was further purified by crystallization from hot ethanol. Yield = 14.8 g (96%). 1H NMR (400 MHz, CDCl$_3$) δ: 7.48 (s, 2H, Ar_H), 5.65 (s, 1H, Ar_OH), 3.64 (s, 2H, OCH$_3$), 2.78 (t, 2H, Ar_CH$_2$CH$_2$), 2.54 (t, 2H, CH$_2$_CH$_2$COOCH$_3$). 13C NMR (100 MHz, CDCl$_3$) δ: 172.77, 152.04, 139.00 (4C), 136.56, 82.15, 51.74, 35.74, and 28.79. MALDI-TOF: MW = 432.0 and m/z = 470.89 (M$^+$ + K$^+$).

3.3.4.3 Synthesis of Methyl-3-(4-(hexadecyloxy)-3,5-diiodophenyl)propanoate (4a)

2(3.0 g, 6.9mmol) and anhydrous K$_2$CO$_3$ (0.95g, 6.9mmol) were dissolved in dry acetonitrile (50 mL) and then heated to 80ºC under nitrogen atmosphere for 1 h. Subsequently, 2-ethylhexyl bromide (3.1g (3.15mL), 10.35mmol) was slowly added into the reaction mixture for 15 min. The reaction was continued for 24 h at 80ºC under nitrogen atmosphere. The reaction mixture was poured into the water and extracted with ethyl acetate. The organic layer was washed with 5% NaOH, brine, and water and then dried with anhydrous Na$_2$SO$_4$. The solvent was evaporated to get yellow liquid as product. It was purified by passing through silica gel column using 2% ethyl acetate in hexane as eluent. Yield =3.48 g (73%). 1H NMR (400MHz, CDCl$_3$) δ: 7.60(s, 2H, Ar_H), 3.94(t, 2H Ar_OCH$_2$), 3.69(s, 3H, COOCH$_3$), 2.83(t, 2H, Ar_CH$_2$ CH$_2$), 2.59(t, 2H, CH$_2$COOCH$_3$), 1.90 (quin, 2H,Ar_OCH$_2$CH$_2$),1.31(m, 26H, RCH$_2$R), 0.90(t,3H, RCH$_3$). 13C-NMR (100 MHz, CDCl$_3$) δ: 172.70, 156.49, 141.14, 140.05, 139.60, 90.85, 73.42, 51.75, 35.26, 31.92, 29.70, 26.95, 22.68, and 14.12.

MALDI-TOF: MW = 656.12 and m/z = 695.15 (M$^+$ + K$^+$).

3.3.4.4 Synthesis of Methyl-3-(4-(dodecyloxy)-3,5-diiodophenyl) propanoate (4b). 2(3.0 g, 6.9mmol) and anhydrous K_2CO_3 (1.05g, 7.59mmol) were dissolved in dry acetonitrile (50 mL) and then heated to 80 ºC under nitrogen atmosphere for 1 h. Subsequently, dodecylbromide (2.58 g, (2.5 mL), 10.35mmol) was slowly added into the reaction mixture for 15 min and remaining procedure was same as 4a. Yield = 2.9 g (70%). 1H NMR (400MHz, CDCl$_3$) δ: 7.60(s, 2H, Ar_H), 3.94(t, 2H Ar_OCH$_2$), 3.69(s, 3H, COOCH$_3$), 2.83(t, 2H, Ar_CH$_2$ CH$_2$), 2.59(t, 2H, CH$_2$COOCH$_3$), 1.90 (quin, 2H,Ar_OCH$_2$CH$_2$),1.31(m, 18H, RCH$_2$R), 0.90(t,3H, RCH$_3$). 13C-NMR (100 MHz, CDCl$_3$) δ: 172.81, 156.56, 140.15, 139.70, 139.28, 90.86, 73.52, 51.86, 35.36, 32.01, 29.73, 29.13, 26.05, 22.79, and 14.23. MALDI-TOF: MW = 600 and m/z = 639.10 (M$^+$ + K$^+$).

3.3.4.5 Synthesis of Methyl-3-(4-(octyloxy)-3,5-diiodophenyl)propanoate (4c). (2.0 g, 4.6mmol) and anhydrous K_2CO_3 (0.7g, 5.06mmol) were dissolved in dry acetonitrile (50 mL) and then heated to 80ºC under nitrogen atmosphere for 1 h. Subsequently, octyl bromide (1.33 g, (1.18mL), 6.9mmol) was slowly added into the reaction mixture for 15 min. Remaining procedure was same as 4a. Yield = 1.75g (70%). 1H NMR (400MHz, CDCl$_3$) δ: 7.60(s, 2H, Ar_H), 3.95(t, 2H Ar_OCH$_2$), 3.69(s, 3H, COOCH$_3$), 2.83(t, 2H, Ar_CH$_2$ CH$_2$), 2.59(t, 2H, CH$_2$COOCH$_3$), 1.89 (quin, 2H,Ar_OCH$_2$CH$_2$),1.31(m, 10H, RCH$_2$R), 0.90(t,3H, RCH$_3$).
MALDI-TOF: MW = 544.21 and m/z = 583.20 (M$^+$ + K$^+$).

3.3.4.6 Synthesis of Methyl-3-(4-(butyloxy)-3,5-diiodophenyl)propanoate (4d). 2(3.0 g, 6.9mmol) and anhydrous K_2CO_3 (1.05g, 7.59mmol) were dissolved in dry acetonitrile (50mL) and then heated to 80ºC under nitrogen atmosphere for 1 h. Subsequently, butylbromide (1.40g, (1.1mL), 10.35mmol) was slowly added into the reaction mixture for 15 min. Remaining procedure was same as 4a.Yield = 2.67g (79%). 1H NMR (400MHz, CDCl$_3$) δ: 7.60(s, 2H, Ar_H), 3.95(t, 2H Ar_OCH$_2$), 3.68(s, 3H, COOCH$_3$), 2.83(t, 2H, Ar_CH$_2$ CH$_2$), 2.59(t, 2H, CH$_2$COOCH$_3$), 1.89 (quin, 2H,Ar_OCH$_2$CH$_2$), 1.60 (quin, 2H,Ar_OCH$_2$CH$_2$), 0.90(t,3H, RCH$_3$). 13C-NMR (100 MHz, CDCl$_3$) δ: 172.60, 156.57, 140.16, 139.71, 139.28, 90.94, 73.23, 51.86, 35.35, 32.19, 29.13, 19.12 and 14.13. MALDI-TOF: MW = 487.90 and m/z = 526.89 (M$^+$ + K$^+$).

3.3.4.7 Synthesis of 3-(4-(hexadecyloxy)-3,5-diiodophenyl)propanoic acid (L16): 4a(4.36g, 6.38mmol) was dissolved in methanol (60 mL) and NaOH(0.4g, 9.57 mmol) in water was added in the mixture. The reaction mixture was refluxed for 12 h and then poured into water. Subsequently, conc. HCl was added to the solution after which white precipitate was formed which was then washed with water until pH became neutral. Yield = 3.46g (85%). 1H NMR (400MHz, CDCl$_3$) δ: 7.62(s, 2H, Ar_H), 3.94(t, 2H Ar_OCH$_2$), 2.84(t, 2H, Ar_CH$_2$ CH$_2$), 2.65(t, 2H, CH$_2$COOCH$_3$), 1.55 (quin, 2H,Ar_OCH$_2$CH$_2$),1.31(m, 26H, RCH$_2$R), 0.89(t,3H, RCH$_3$). 13C-NMR (100 MHz, CDCl$_3$) δ: 177.83, 156.68, 139.70, 91.03, 73.55, 35.15, 32.02, 29.80, 26.05, 22.79 and 14.23. MALDI-TOF: MW = 642 and m/z = 681.03 (M$^+$ + K$^+$).

3.3.4.8 Synthesis of 3-(4-(dodecyloxy)-3, 5-diiodophenyl)propanoic acid (L12): 4b(3g, 5mmol) was dissolved in methanol (50 mL) and NaOH(0.3g, 7.5mmol) in water was added in the mixture. Remaining procedure was same as that of L16 Yield = 2.62g (90%)**.** 1H NMR (400MHz, CDCl$_3$) δ: 7.62(s, 2H, Ar_H), 3.94(t, 2H Ar_OCH$_2$), 2.84(t, 2H, Ar_CH$_2$ CH$_2$), 2.65(t, 2H, CH$_2$COOCH$_3$), 1.90(quin, 2H,Ar_OCH$_2$CH$_2$),1.54(quin, 2H,Ar_OCH$_2$CH$_2$) ,1.31(m,18H, RCH$_2$R) and 0.89(t,3H, RCH$_3$). 13C-NMR (100 MHz, CDCl$_3$) δ: 177.83, 156.68, 139.70, 91.01, 73.55, 35.00, 32.01, 29.73, 26.05, 22.78 and 14.22. MALDI-TOF: MW = 586.04 and m/z = 608.93 (M$^+$ + Na$^+$).

3.3.4.9 Synthesis of 3-(4-(octyloxy)-3, 5-diiodophenyl)propanoic acid (L8): 4c(2g, 3.8mmol) was dissolved in methanol (30mL) and NaOH(0.23g, 5.7mmol) in water was added in the mixture. Remaining procedure was same as that of L16. Yield = 1.83g (91%). 1H NMR (400MHz, CDCl$_3$) δ: 7.62(s, 2H, Ar_H), 3.94(t, 2H Ar_OCH$_2$), 2.84(t, 2H, Ar_CH$_2$ CH$_2$), 2.65(t, 2H, CH$_2$COOCH$_3$), 1.91(quin, 2H,Ar_OCH$_2$CH$_2$),1.55(quin, 2H,Ar_OCH$_2$CH$_2$) ,1.31(m, 10H, RCH$_2$R) and 0.90(t,3H, RCH$_3$). 13C-NMR (100 MHz, CDCl$_3$) δ: 177.53, 156.68, 139.77, 91.01, 73.55, 31.96, 30.10, 29.57, 26.05, 22.77 and 14.21. MALDI-TOF: MW = 529.98 and m/z = 568.83 (M$^+$ + K$^+$).

3.3.4.10 Synthesis of 3-(4-(butyloxy)-3, 5-diiodophenyl)propanoic acid (L4): 4d(2.67g, 5.47mol) was dissolved in methanol (30mL) and NaOH(0.33g, 8.21mmol) in water was added in the mixture. Remaining procedure was same as that of L16. Yield = 2.50g (97%). 1H NMR (400MHz, CDCl$_3$) δ: 7.62(s, 2H, Ar_H), 3.95(t, 2H Ar_OCH$_2$),

2.84(t, 2H, Ar_CH$_2$ CH$_2$), 2.65(t, 2H, CH$_2$COOCH$_3$), 1.89(quin, 2,Ar_OCH$_2$CH$_2$),1.58(quin, 2H,Ar_OCH$_2$CH$_2$) , and 1.02(t,3H, RCH$_3$).

MALDI-TOF: MW = 473.92 and m/z = 512.77 (M$^+$ + K$^+$).

3.3.4.11 Synthesis of Methyl-3-(3,5-diiodo-4methoxyphenyl) propanoate (3).2 (2.0 g, 4.6mmol) and KOH (0.4 g, 6.95mmol) were dissolved in DMSO (10mL) after which methyl iodide (1.08g, 0.5ml, 6.95mmol) was added dropwise. The reaction was continued at room temperature under nitrogen atmosphere for 24 hours. The reaction mixture was poured into the water and extracted with dichloromethane. The organic layer was washed with 5% NaOH, brine and water and then dried over anhydrous Na$_2$SO$_4$. The solvent was evaporated to get yellow solid as product. It was purified by passing through silica gel column using hexane and 5% ethyl acetate as eluent to give white crystalline powder as product after evaporating solvent. Yield =1.45g (70%). 1H NMR (400MHz, CDCl$_3$) δ: 7.61(s, 2H, Ar_H), 3.84(s, 3H Ar_OCH$_3$), 3.69(s, 3H, COOCH$_3$), 2.83(t, 2H, Ar_CH$_2$ CH$_2$), and 2.59(t, 2H, CH$_2$COOCH$_3$). 13C NMR (100 MHz, CDCl$_3$) δ: 171.67, 157.27,140.37, 139.60, 90.39, 60.67, 51.77, 32.22, and 20.02. MALDI-TOF: MW = 445.89 and m/z = 484.12 (M$^+$ + K$^+$).

3.3.4.12 Synthesis of 3-(3,5-diiodo-4-methoxyphenyl)propanoic acid (L1): 3(1.5 g, 3.4 mmol), was dissolved in methanol (20 mL) and NaOH (0.27g, 6.8mmol) in water was added in the mixture. The reaction mixture was refluxed for 12 h and then poured into water. Subsequently, conc. HCl was added to the solution after which white precipitate was formed which was then washed with water until become pH neutral. Yield = 1.25g (85%). 1H-NMR (400 MHz, CDCl$_3$) δ: 7.70 (s, 2H, Ar - **H**), 3.79 (s, 3H, OC**H**3), 2.81 (t, 2H, Ar-C**H**2CH2), 2.53 (t, 2H, - CH2C**H**2-COOCH3). 13C-NMR (100 MHz, CDCl$_3$) δ: 174.90, 157.38, 141.14, 139.71, 89.60, 59.79, 34.91 and 28.70. MALDI-TOF: MW = 431.99 and m/z = 452.97(M$^+$ + Na$^+$).

4. RESULTS AND DISCUSSION
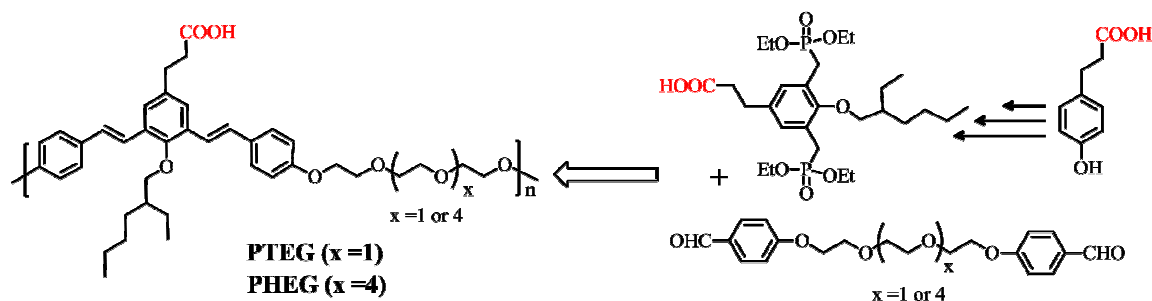
4.1 Synthesis of Segmented Polymer

Fig 4.1 PTEG and PHEG polymer structure

Two segmented polymers PTEG and PHEG were synthesized having identical distilbene chromophore with triethylene glycol (TEG) and hexaethylene glycol (HEG) units as spacers in the main chain (see Figure 4.1). The carboxylic functionalized distilbene chromophore design was adopted based on our previous experience on the π-conjugated polymer photosensitizers.[4] Earlier investigation on the above polymer design revealed that carboxylic functionalized distilbene polymer design was very crucial for achieving temperature sensing in polymer-Eu^{3+} complex in both solution and solid state.[4] Phenylpropionic acid was used as starting material and polymers were made through multi-step synthesis (from previous reports).
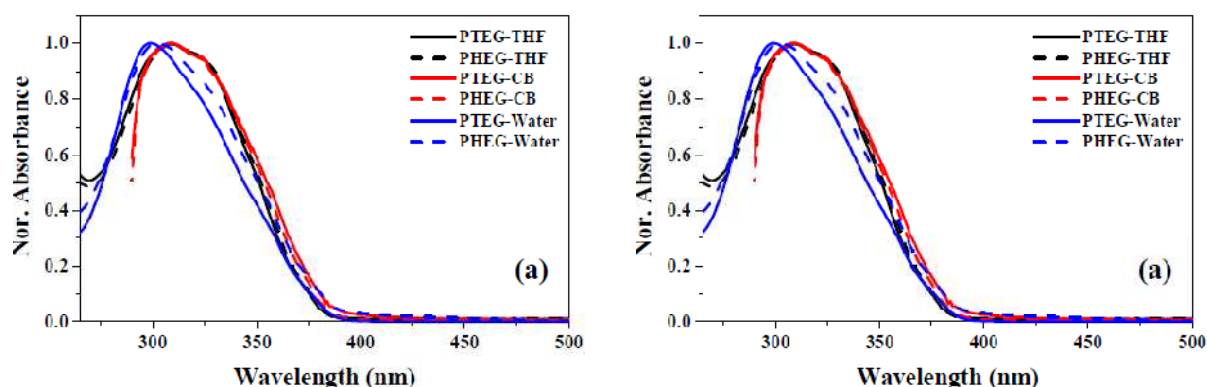

Fig 4.2 Absorption and emission spectra of polymers in different solvents

The molecular weight of the polymers were obtained as M_n = 8000 - 8300 and M_w = 16000 – 24000. The carboxylic acid group was converted into their sodium salts for

sensing. The absorbance and emission spectra of the polymers exhibited maxima at 310 nm and 410 nm, respectively (see figure 4.2)

4.2 Temperature sensing: The probe was developed using the polymer PHEG (also PTEG) in complexation with Eu^{3+} ions.[4] The polymers were found to be a selective photosensitizer to Eu^{3+} ions compared to other lanthanides. The polymer ligand to metal-ion excitation energy transfer (LMET) showed characteristic Eu^{3+} strong metal centered sharp emission (λ_{ex} =350 nm) peaks at 580, 593, 614, 650 and 702 nm corresponding to various D$\rightarrow$ F transitions[4] (see figure 4.3a at 20 °C). The photograph of polymer-Eu^{3+} complex (in figure 4.3) showed strong red emission in solution confirming the complete excitation energy transfer from blue-emitting π-conjugated distilbene polymer backbone. The occurrence of LMET process in the complexes was validated from their singlet and triplet energies polymeric ligands and the excited energy levels of Eu^{3+} ions (figure 4.4).
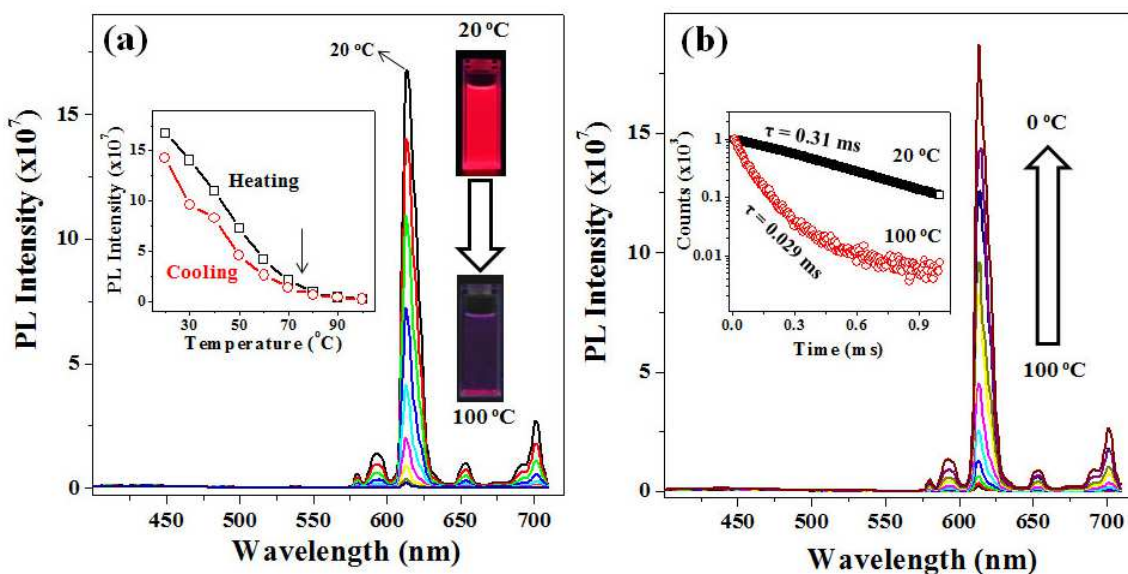

Fig 4.3 Temperature probe of PHEG-Eu^{3+} complex at $1.8x10^{-6}$ M (repeat unit concentration) in the heating (a) and cooling (b) cycles (in chlorobenzene). The in-set in (a) showed the plots of PL intensity at temperatures (λ_{ex} =350 nm). The in-set in (b) showed the TCSPC profiles of polymer-Eu^{3+} at 20° and 100°C.

30

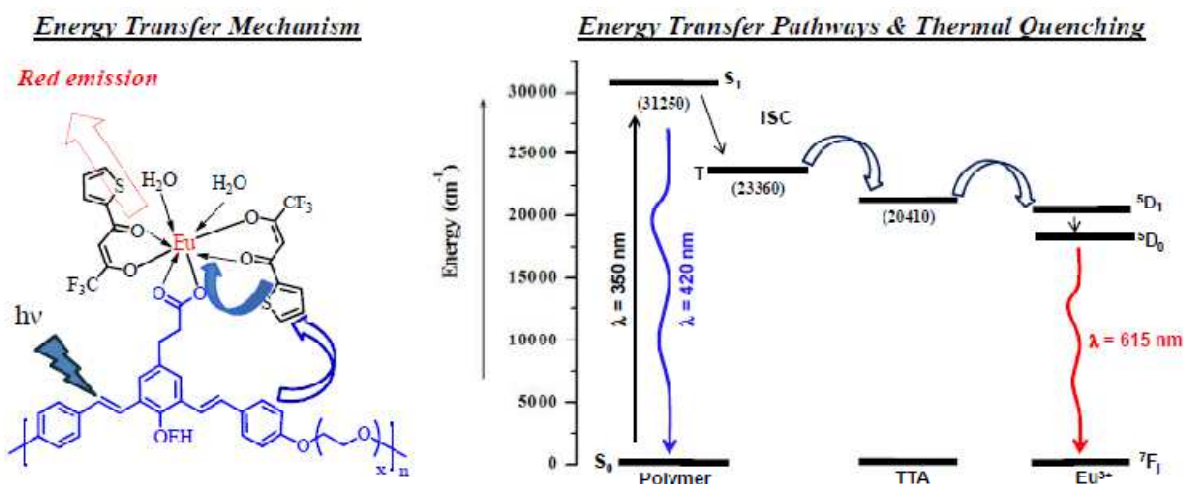*Fig 4.4 Schematic diagram for the energy transfer pathways in segmented polymer-Eu^{3+} complexes.*

The polymer-Eu^{3+} ion complex showed unique temperature sensing in chlorobenzene, THF, DMSO, p-xylene and so on. The strong and sharp red-emission at 20 °C was gradually diminished while heating up to 100 °C (see figure 4.3a, in chlorobenzene). In the subsequent cooling cycle, the red emission recovered completely while cooling from 100 to 20 °C (see figure 4.3b). The FL-intensities of the red-emission at 615 nm were plotted against the temperature and shown as in-set in figure 4.3a. The temperature turn-On and turn-Off switch was found to work at 72 °C (shown by arrow). The temperature sensing ability of the PHEG-Eu^{3+} ion complex arose by the destabilization of Eu^{3+}ion excited state ($^5D_0$ states) at higher temperatures[26, 27] (see energy level in figure 4.4). TCSPC profiles for PHEG-Eu^{3+} are given as in-set in figure 4.3b (λ_{ex} =350 nm and collected at 612 nm). The lifetime of the excited species were found to be 3.1 ms at 20 °C whereas it drastically decreased to 21 μs at 100 °C. The decay profiles were also found to be completely reversible in the subsequent cooling cycles. Thus, the thermo-sensitive probe of polymer-Eu^{3+} ions complexes worked by two processes: (i) turn-On via LMET from the polymer to Eu^{3+} ions and (ii) turn-Off through the destabilization of $^5D_0$ excited states of the metal-centre.

4.3 Metal-ion sensing: It was performed in PIPES buffer at pH 7.4. The absorption spectra of the polymers showed 8-10 nm blue shift with increase in the concentrations of Cu^{2+} ion. Up on the addition of metal ions into the sodium salt of the polymers, the metal complex formed with carboxylate anion by displacing the sodium ion. This indicated the formation of polymer- Cu^{2+} ion complexes. The fluorescence responses of the PHEG-Na$^+$ polymer at various Cu^{2+} ion concentrations are shown in figure 4.5a.
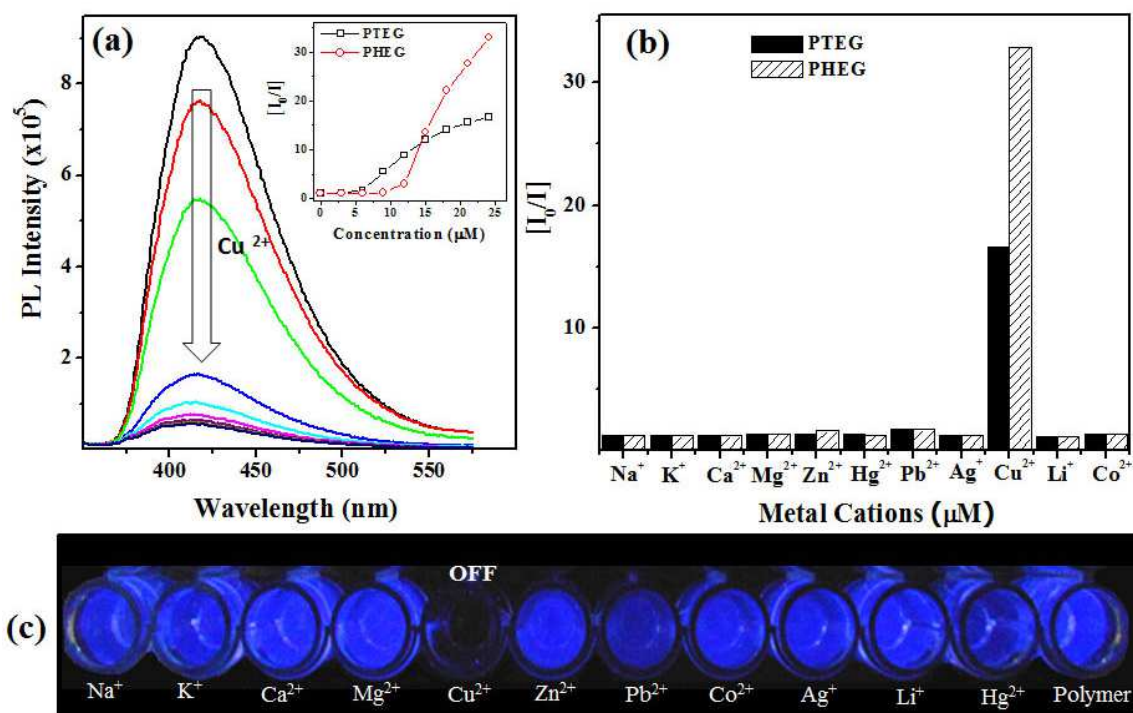
Fig 4.5(a) Emission spectra of PHEG-Na$^+$ in $5x10^{-6}M$ (repeat unit concentration) in PIPES buffer and the concentration of Cu^{2+} ions are varied from 3 µM to 24 µM in PIPES buffer (λ_{ex} = 310 nm). The in-set in (a) showed the plots of I_o/I variation over the concentration of Cu^{2+}ions. (b) I_o/I values for various metal ions at 24 µM in PIPES buffer. (c) Photographs of vials.

The polymer emission was found to quench drastically with the increase in Cu^{2+} ion concentrations. The polymer showed complete quenching (more than 97 %) at 24µM of Cu^{2+} ion indicating their upper detection limit. The fluorescence turn-off switch in these π-conjugated systems towards Cu^{2+} ion was attributed to the quenching of excitation energy by the metal-ions through heavy atom effect.[29] The lower detection limits of both

PTEG and PHEG polymers for Cu^{2+} metal ion were found as 3µM. To further quantify the turn-Off efficiencies of these polymers, the fluorescence intensity of the polymers at Cu^{2+} ion at various concentrations were fitted into the Stern-Volmer equation: $I_o/I = 1+K_{sv}[Cu^{2+}]$, where I_o and I are the initial and final emission intensity of the chromophores and K_{sv} is the Stern-Volmer quenching constant.[30] The inset figure of 4.5a, showed the Stern-Volmer plots of polymers for Cu^{2+} ion. The plots exhibited a typical non-linear trend with respect to both static and dyanamic fluorescence quenching towards the analytes. The Stern-Volmer constants were obtained as 6.1×10^5 M^{-1} and 4.5×10^5 M^{-1} for PTEG and PHEG polymers, respectively. The K_{sv} values from the polymer probes are comparable to that of other probes reported for Cu^{2+} ion sensing.[31, 32]

The selectivity of the polymer probes towards Cu^{2+} ions over other metal cations were also tested (see figure 4.5b). The fluorescence quenching experiments were carried out for more than 12 metal cations from alkali and transition groups: Na^+, K^+, Li^+, Ca^{2+}, Mg^{2+}, Pb^{2+}, Ag^+, Zn^{2+}, Hg^{2+}, and Co^{2+} ions in PIPES buffer solutions at pH 7.4. The fluorescence responses of the polymers at 24 µM Cu^{2+} ions concentrations are shown in figure 3.5c. The bar diagram (figure 4.5b) showed further evidence that most of these metal ions showed very little to negligible sensing comparable to the super-quenching observed in Cu^{2+} ion. It is rather clear in figure 4.5b that fluorescence quenching efficiency of polymers by Cu^{2+} ions is nearly 20-30 times higher as compared to other metal ions. The selectivity of polymer towards the Cu^{2+} ion can be clearly seen in the photograph shown in figure 4.5c. These results suggest that both PTEG and PHEG have good selectivity towards Cu^{2+} ion even in the presence of other alkali, alkaline, heavy and transition metal ions. Further, the polymer probes did not show any interference with other divalent transition metals (Pb(II) or Hg(II) ions)[32] and showed high selectivity towards Cu^{2+} ions in water. The sensing ability of the polymer probe also showed remarkable difference with respect to the number of oligoethyleneoxy units in the backbone. The effect of hexaethyleneoxy spacer polymer (PHEG) was found to be almost twice compared to triethyleneoxy chain counterparts (PTEG) (see the data in figure 4.5b). This difference is attributed to the ability of the distilbene chromophores in polymer backbone to scavenge the metal-ions. Longer segmented spacer provide more

degree of flexibility for the distilbene chromophores to wrap around the Cu^{2+} ion which is relatively less preferred in the shorted segments.

4.4 Biomolecule sensing: The probe was tested based on the turn-On ability of the quenched polymer-Cu^{2+} by biological molecules. This turn-On switch was investigated for anions such as phosphates and variety of L-amino acids. Amino acids disrupt the polymer-Cu^{2+} complex (turn-Off switch) in aqueous medium by strongly complexing with Cu^{2+} ions compared to carboxylate distilbene chromophores in the polymer backbone. The completely fluorescence quenched polymer (95 %) solutions containing 24 μM of Cu^{2+} in PIPES buffer (at pH = 7.4) was chosen as device for sensing the amino acids. The quenched solution regained florescence to different extents upon adding amino acids to it. 6 different amino acids were tried based on different functionalities they had and their response is given in figure 4.6b. The sensing by tryptophan 30 and glutamine were second best compared to histidine. Alanine, cysteine and serine showed relatively weak sensing capabilities. This revealed that heterocyclic ring in histidine bind more strongly to Cu (II) ions (shown in figure 4.6a) compared to than other functional groups in amino acids.
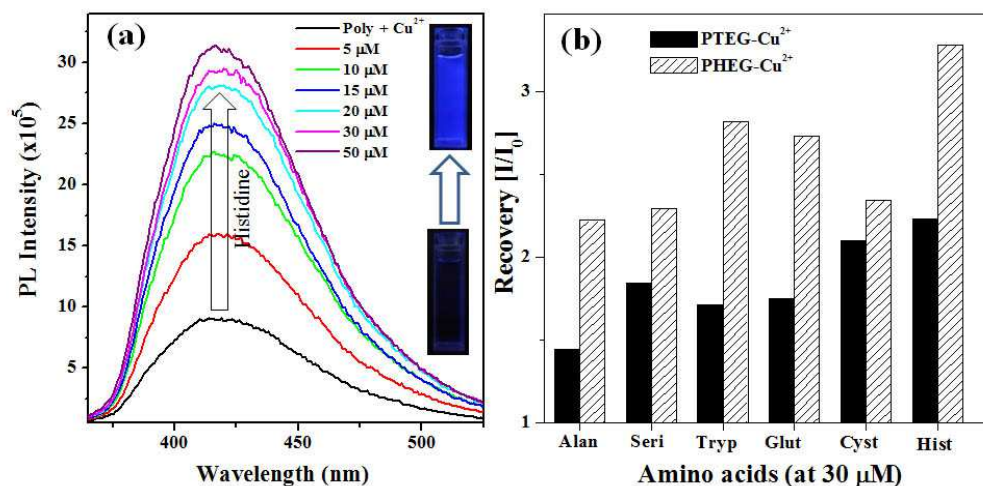

Fig 4.6 (a) Fluorescence response from the PHEG-Cu^{2+} ion complex (using 5×10^{-6}M of PHEG-Na^+ and 24 μM of Cu^{2+} ion) upon the addition of histidine from 5 to 50 μM in PIPES buffer (λex = 310 nm). (b) I/I0 values for various amino acids at 30 μM

Limitation of Co-ligand complexation

For the development of these kind of molecular probes into device making to take care of needs of society, processibility and sensitivity of such probes is an issue. Because of the need of a co-ligand in such europium complexes for sensitizing it, the sensitivity of such probes decreases because of stray emission of co-ligand and the sensing behavior of the probes are no longer ratiometric. Taking care of these issues, 5 ligands as mentioned in general procedure section and their europium complexes were synthesized which sensitized europium metal ion without any co-ligand and some of the complexes were soluble in organic solvent making them easy to process.

4.5 Designing of new organic ligands for lanthanides

Five different ligands designated as L16, L12, L8, L4 and L1 were synthesized rationally which had the same chromophore unit but different alkyl chains substituted at the phenol's hydroxyl proton. All the ligands and their precursors were characterized using 1H NMR, 13C NMR and MALDI-TOFF. Figure 4.8 shows the synthetic scheme of all the ligands.
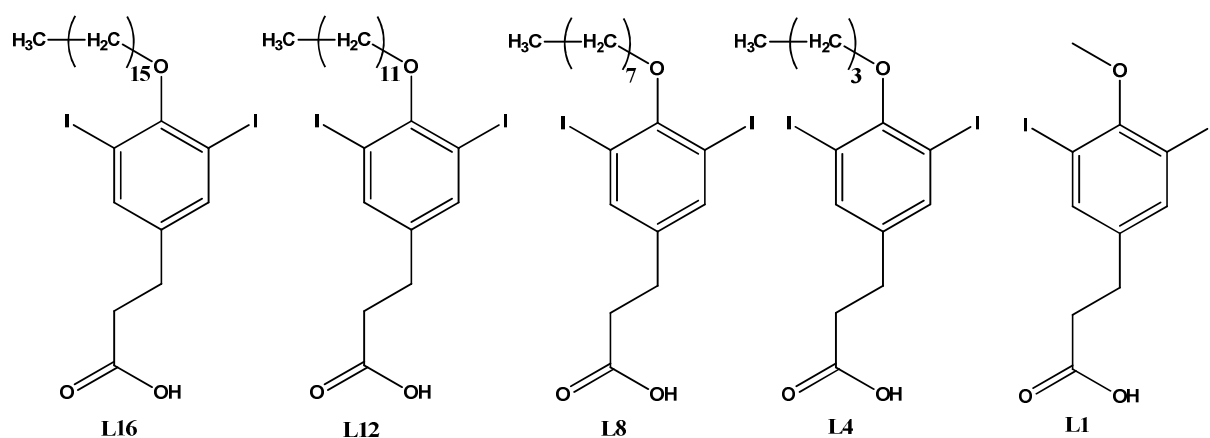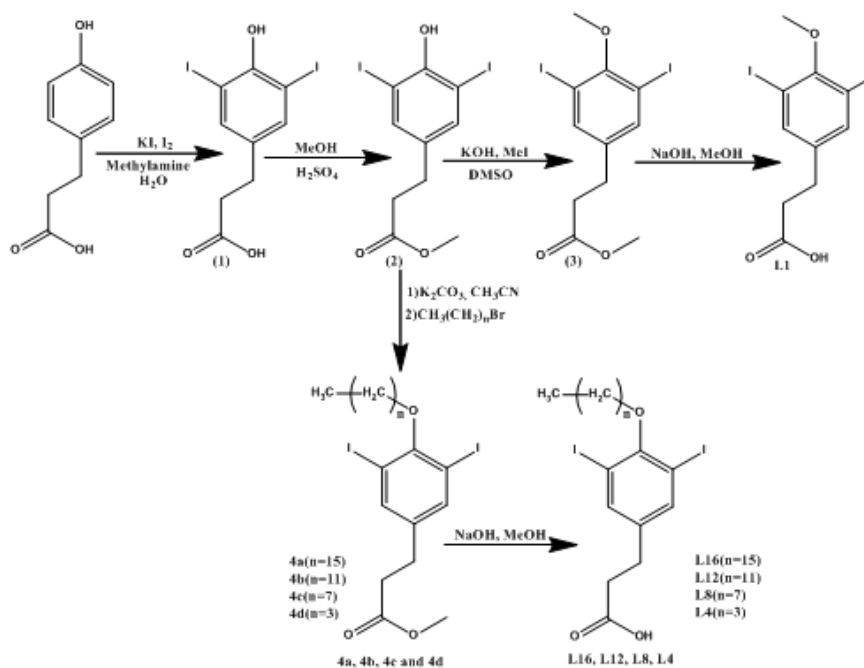

Fig 4.7 Organic ligands for sensitizing Europium metal

Fig 4.8 Synthetic scheme of ligands

4.6 Thermal study of ligands

The ligands L4, L8, L12 and L16 were subjected for Thermo gravimetric analysis which showed that they were stable up to 290°C after which it decomposed. Taking care of the fact that they decomposed at around 300°C, all ligands were then subjected for Differential Scanning Calorimetry studies from -50°C to 150°C as shown in figure 4.9
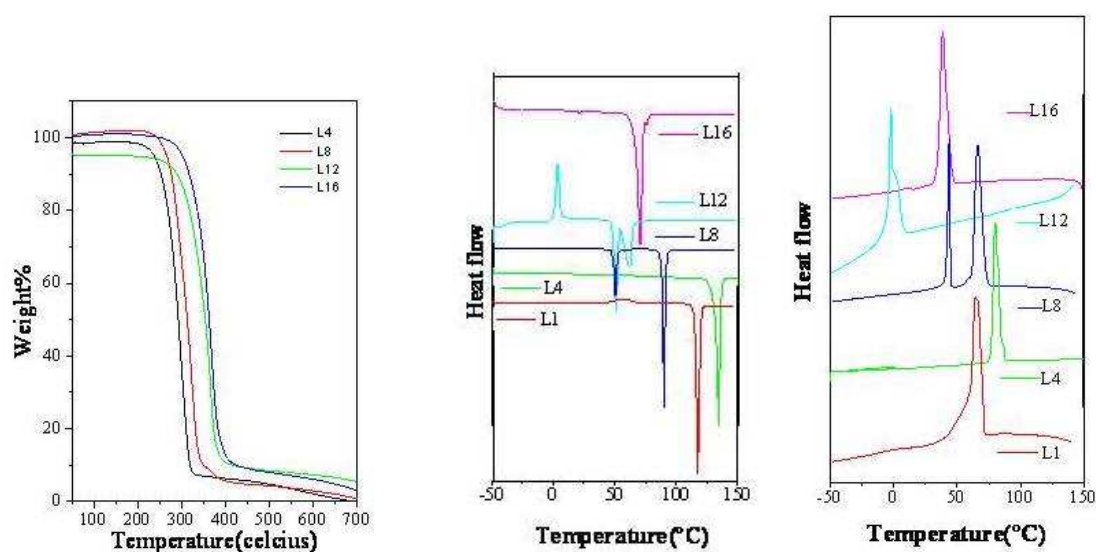

Fig 4.9 TGA profile (a), DSC profile while heating (b) and DSC profile(c) while cooling of ligands

36

Each of the ligand had a characteristic melting temperature which randomly varied with an increase in alkyl chain length.
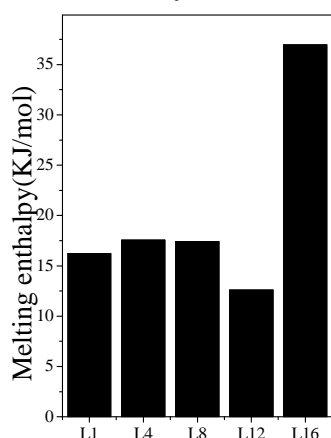

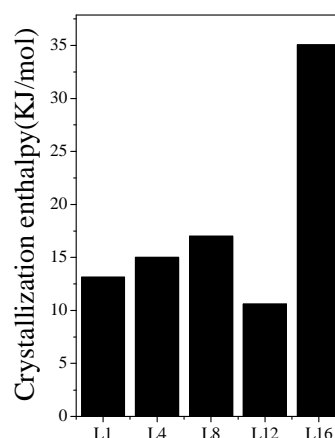*Fig 4.10 Enthalpy of melting of ligands*

Fig 4.11 Enthalpy of crystallization of ligands

The enthalpy of melting value for each ligand suggested the degree to which each ligand was packed. L1, L4, L8 and L12 had almost similar values but in case of L16 the enthalpy value was almost double to the other values which indicated that the degree of packing in case of L16 (figure 4.10) was highest because of the extremely long chain which promoted the Vander Wall's interaction between alkyl chains leading to very effective packing of such molecules. Similarly the DSC profile of ligands while cooling gave the enthalpy value of crystallization (figure 4.11). The enthalpy of crystallization also followed the same trend where L1, L4, L8 and L12 had the same value while in case of L16 the enthalpy value was almost double which indicated its high extent of packing while undergoing controlled cooling.

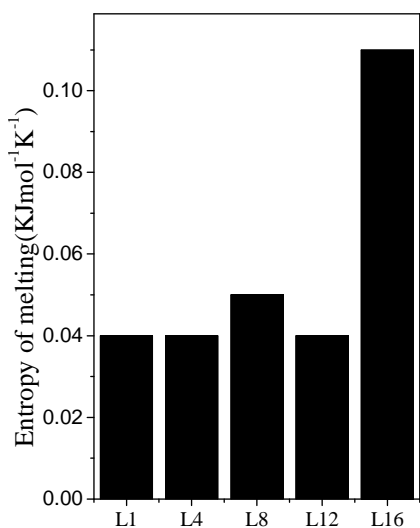| Ligand	$\Delta H_{melting}$ (KJmol^{-1})	$\Delta H_{crystallization}$ (KJmol^{-1})	$\Delta S_{melting}$ (KJmol^{-1}K^{-1})	$\Delta S_{crystallization}$ (KJmol^{-1}K^{-1})
L1	16.23	13.12	0.04	0.04
L4	17.56	15.01	0.04	0.04
L8	17.40	17.00	0.05	0.05
L12	12.59	10.61	0.04	0.04
L16	36.97	35.07	0.11	0.11

Table 4.1 Enthalpy and Entropy values

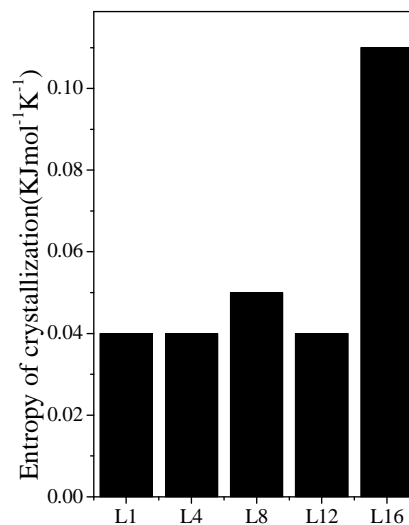Fig 4.12 Entropy of melting of ligands   Fig 4.13 Entropy of crystallization

The entropy value was also calculated at respective melting and crystallization temperature and it suggested the same trend with the value remaining nearly constant on moving from L1 to L12 gradually but was twice in case of L16(figure 4.12 and 4.13) which is in sync with the packing information available from enthalpy value. The value of melting and crystallization enthalpy and entropy is shown in the table 4.1.

4.7 Emission and lifetime study of ligands

Thermal studies confirmed the extent of packing in each ligand which was highest in case of L16 while in case of L1, L4, L8 and L12 it was not so significant. Considering the fact that we had substituted the heavy atom iodine on the chromophore unit strategically and L16 showed greatest extent of packing, emission studies of each ligand was done to see if they were phosphorescence or not. The emission spectra of ligands upon excitation at 290 nm was done in chloroform solution but all the ligands showed peaks in the range of 375 nm to 425 nm wavelength region which is corresponding to fluorescence(figure 4.14). There was no extra peak in the emission spectra at higher wavelength region corresponding to phosphorescence. This fits very well with the rational relation between packing of molecules and phosphorescence generation. In solution, molecules of ligand are separated far away from each other

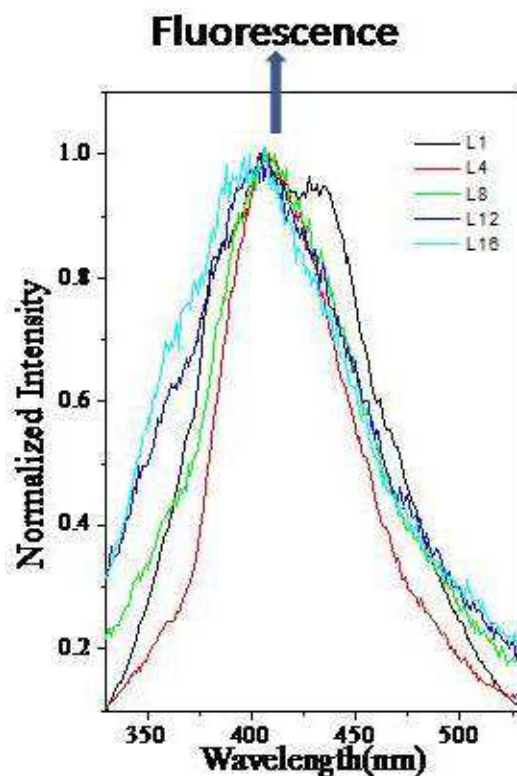which prevents iodine molecule from coming close to the chromophore unit therby restricting the heavy atom effect

Fig 4.14 Emission spectra of ligands in solution

Furthermore, emission study of ligands was done in powdered state which is shown in figure 4.16. Emission spectrum of ligands upon excitiation at 330 nm in powdered state (figure 4.16) was in stark contrast with the emission spectra in solution. Ligands L1, L4 and L8 showed peaks in the range of 375 nm to 450 nm which is characteristic of fluorescence while ligands L12 and L16 showed extra peaks at around 515 nm and 554 nm that is characteristic of phosphorescence. In L12 and L16 molecules having long alkyl chains pack strongly because of strong vander walls interactions which brings heavy atom iodine near to the chromophore unit which leads to the spin orbit coupling bringing excited electrons in the triplet state from the singlet state. The excited electrons then undergo radiative decay to the ground state showing the phosphorescence peak at higher wavelength region.
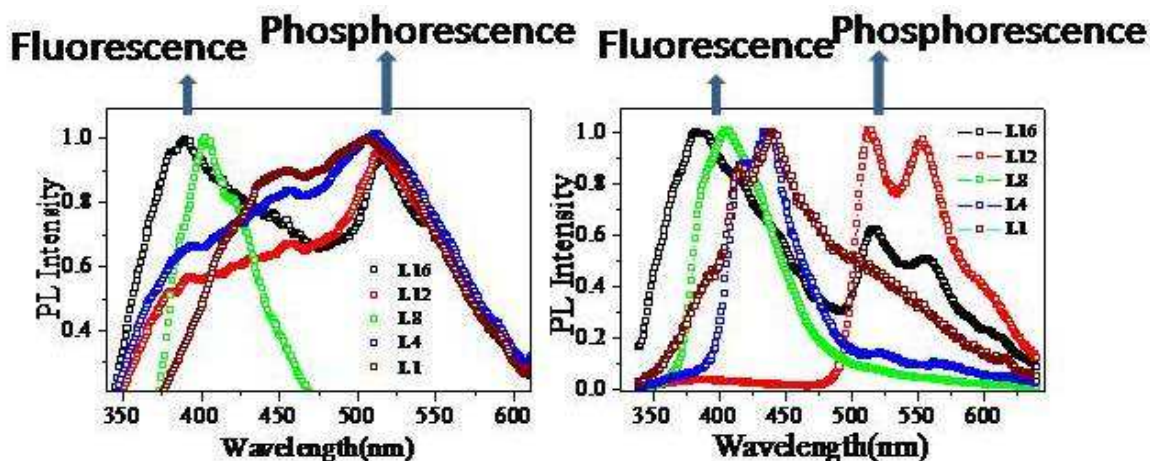
Fig 4.15 Emission of ligands in annealed state   Fig 4.16 Emission of ligands in powdered state

But the solid state emission spectra of L12 and L16 showed peak corresponding to fluorescence also which suggests that there was not complete transfer of excited state electrons from singlet to triplet state but rather a fraction of electrons were transferred. The exact contribution in phosphorescence coming from each ligand can be calculated using the absolute phosphorescence quantum yield calculation. To further see the effect of packing on emission spectra, solid samples were first heated and then cooled in a controlled fashion on polarized light microscopy (PLM) slides. This led to the annealing of samples which were crystalline as shown in figure 3.17.
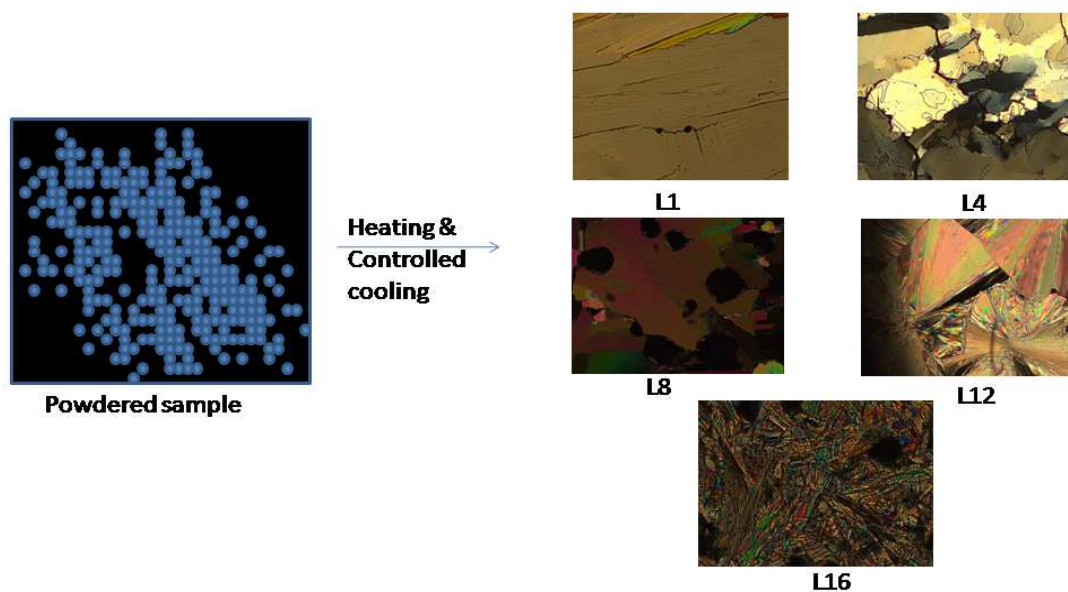

.   Fig 4.17 Images of annealed ligands taken from PLM

The emission spectra of annealed samples sandwiched in between the PLM slides was also taken by exciting the ligands at 330 nm which is shown in figure 4.15. Emission spectrum of ligands in annealed state supports the direct relation of packing with phosphorescence. After annealing, all the ligands except L8 showed the phosphorescence peak at higher wavelength region of 520 nm. Upon controlled cooling each of the ligand packs much more effectively as compared to the powdered state which leads to more pronounced heavy atom effect because of iodine which initiates the triplet state excited electrons population generation in case of L1 and L4 also which was otherwise not possible in powder form.

To confirm the fact that the extra peak arising out in case of powdered and aligned samples at higher wavelength in 520 nm region is because of phosphorescence and at lower wavelength is because of fluorescence, time resolved luminescent decay studies of each ligand was carried out using TCSPS technique. The solid state TCSPS profile of ligands with respect to fluorescence (collected at 370 nm to 450 nm by using 339 nm LED as excitation source) and phosphorescence (collected at 517 nm to 560 nm using pulsed Tungsten lamp as excitation source) is shown in figure 4.18 and 4.19 respectively. For L12 and L16 the lifetime corresponding to fluorescence was less than the nanosecond time scale and could not get calculated using the nanosecond time scaled LED.
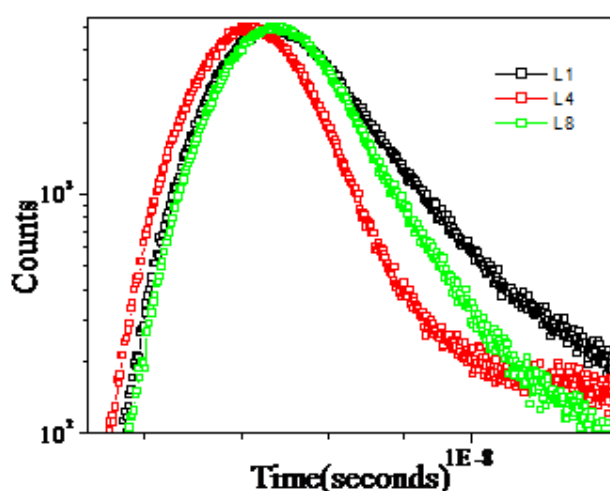

Fig 4.18 TCSPS decay profile corresponding to fluorescence in powdered state

Ligands L1 and L4 were fitted tri exponentially while L8 was fitted bi exponentially to give the decay lifetime in the order of nanoseconds which is given in table 4.2

Ligand	$T_{1fluorescence}$(ns)	$T_{2fluorescence}$(ns)	$T_{3fluorescence}$(ns)
L1	0.50	1.46	7.56
L4	0.18	11.6	2.97
L8	0.48	2.15	-

Table 4.2 Lifetime values for ligands L1, L4 and L8 with respect to fluorescence

The lifetime of each ligand obtained with respect to phosphorescence showed completely opposite trend as compared to lifetime obtained with respect to fluorescence as shown in figure 4.19. Ligands L12 and L16 had the slowest decay which was so fast in case of fluorescence that it could not be calculated using nanosecond time scaled LED while L4 had the fastest decay which is shown in figure 4.15. The respective lifetime values fitted mono exponentially for L4 and L12 and bi exponentially for L16 are each given in table 4.3
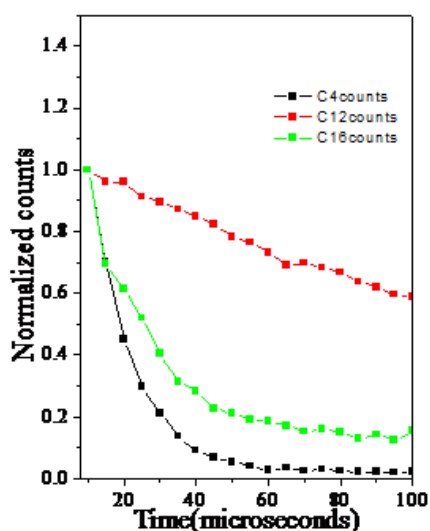
Ligand	T_{1phos}(µs)	T_{2phos}(µs)
L4	12.86	-
L12	185.9	-
L16	18.74	1417

Table 4.3 Phosphorescence lifetime values

Fig 4.19 TCSPS decay corresponding to phosphorescence

In an attempt to see the relative contribution of phosphorescence with respect to fluorescence in the solid state emission spectra of powdered and annealed ligands, the ratio of areas of curves corresponding to phosphorescence and fluorescence was taken which is shown in figure 4.20.
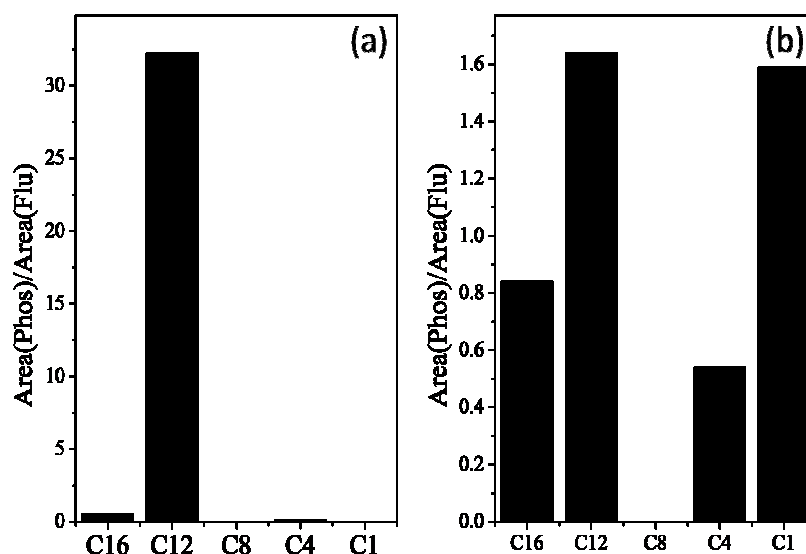
Fig 4.20 Ratio of area of curve corresponding to fluorescence and phosphorescence in a)powdered ligands b)annealed ligands

In powdered ligands L4 and L16 the contribution due to phosphorescence was less than fluorescence while in case of L12 the contribution due to phosphorescence was unusually high. For samples L1 and L8, there was no phosphorescence so the area ratio was zero. But once the samples were annealed there was an increase in the contribution of phosphorescence relative to fluorescence in case of L1 (which was zero in powdered sample), L4 and L16. For L8 in annealed state there was again no phosphorescence while for L12 the contribution of phosphorescence decreased from the previous case. This unusual behavior of L12 can be attributed to the proximity of iodine from chromophore unit which is lower in case of powdered sample as compared to annealed samples.

4.8 Synthesis and characterization of Europium complexes Ligand **(L1 or L4 or L8 or L12 or L16)** was dissolved in minimum amount of ethanol and NaOH (3 equivalents) in water was added into the solution. The solution was made transparent by adding a little amount of DMSO. The whole mixture was stirred well for around 30min till the

solution become homogenous. $Eu(NO_3)_3 \cdot 6H_2O$ (1 equivalent) in ethanol (1mL) was slowly added into the mixture, the precipitate was formed and stirring was continued for 12h. The precipitate was filtered, washed with excess of water and ethanol solution. The white colored complexes were dried under vacuum.
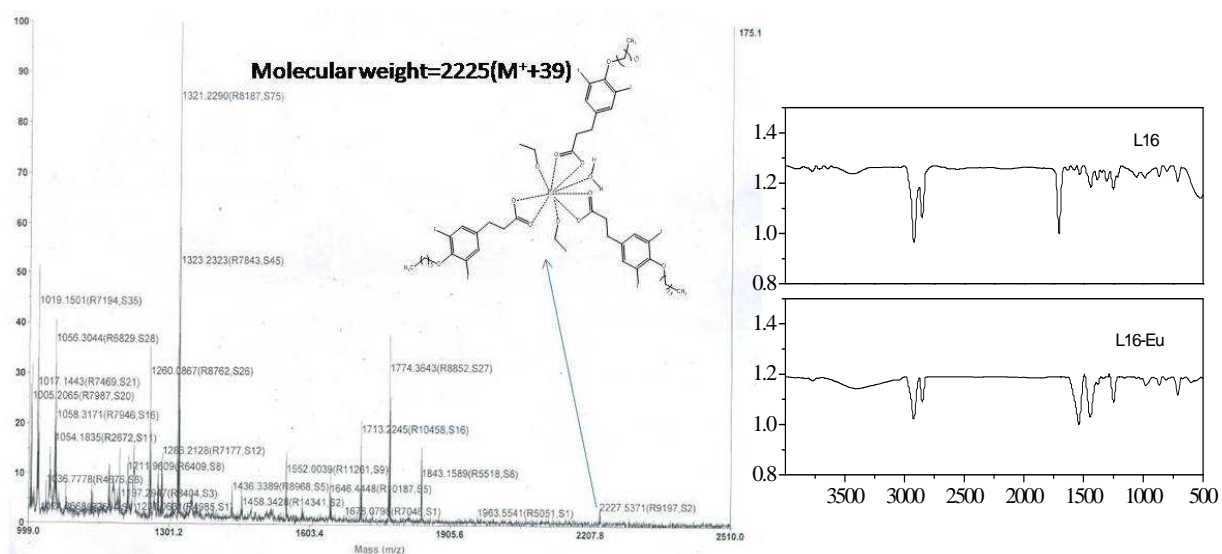

Fig 4.21 MALDI-TOFF and IR characterization of complex

The formation of Eu3+ complexes was confirmed by FT-IR spectroscopy and MALDI-TOF (figure 4.21). The C=O bond stretching frequency around 1705 cm^{-1} of the ligands L1, L4, L8, L12 and L16 disappeared completely in all the Eu^{3+} complexes and appearance of new peaks at 1600 and 1490 cm-1(shown in figure 4.21) corresponding to symmetric and antisymmetric Eu-C=O vibrations were observed as shown in figure. MALDI-TOF analysis showed that Europium was coordinated by 3 molecules of ligand in a bidendate fashion with carboxylic acid and other 3 sites were coordinated by 2 molecule of ethanol and one molecule of water.

4.9 Emission and lifetime study of europium complexes

All europium complxes were red emitting to different extents in solid state under UV illumination. Emission study of the complexes as shown in figure 4.22 was done in solid

state by exciting the complexes at 330 nm which was corresponding to the excitation of ligands in solid state.
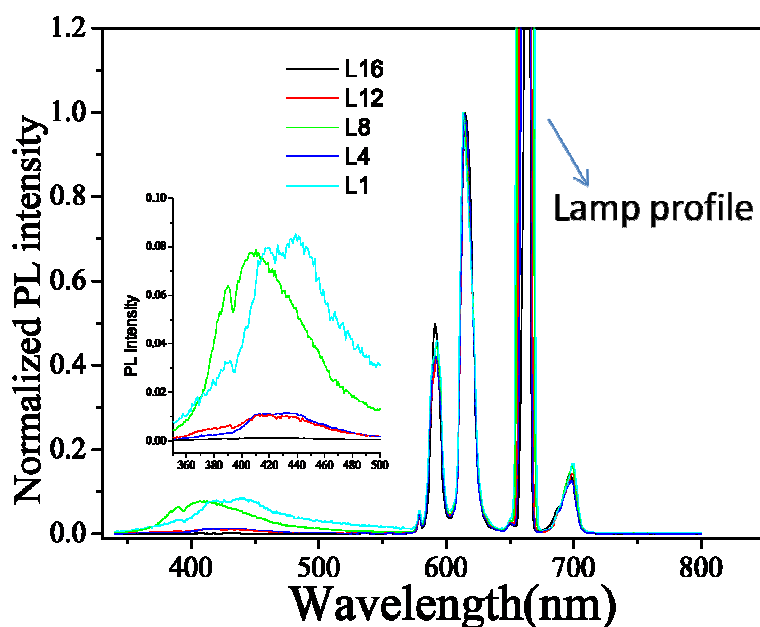

Fig 4.22 Emission spectra of complexes using excitation wavelength of 330 nm

The solid state emission spectra of complexes showed 5 sharp peaks at 580, 592, 615, 650 and 699 nm with respect to $^5D_0 \longrightarrow {}^7F_0$, $^5D_0 \longrightarrow {}^7F_1$, $^5D_0 \longrightarrow {}^7F_2$, $^5D_0 \longrightarrow {}^7F_3$, and

$^5D_0 \longrightarrow {}^7F_4$ transitions of Europium metal ions. The emission intensity of Eu^{3+} complexes was normalized to see the relative emission because of energy transfer from ligand to Europium and self emission because of ligand only (which is shown in the inset of figure4.22). The self emission comes into picture because on exciting the complexes at 330 nm complete energy transfer is not occurring from ligand to metal. A part of excitation energy is absorbed by the ligand itself which leads to the self emission of the ligand. The excitation spectra of the complexes was also taken which showed some sharp excitation peaks corresponding to metal and broad peak from 320 to 350 nm corresponding to ligand as shown in figure 4.23.
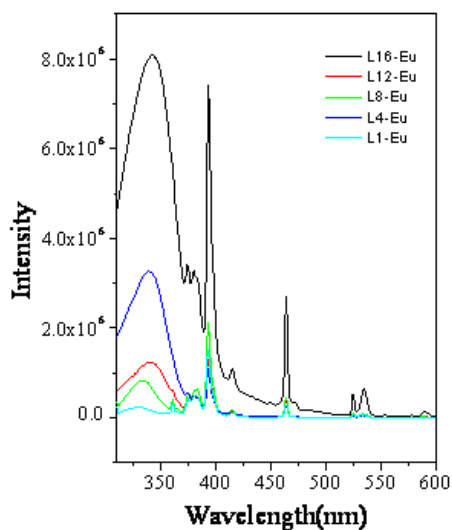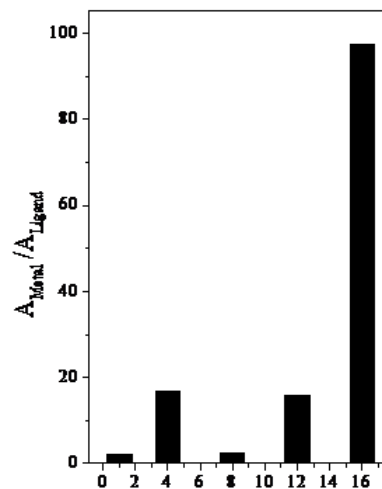
Fig 4.23 Excitation spectra of Europium complexes   *Fig 4.24 Ratio of area under Eu and ligand*

Emission

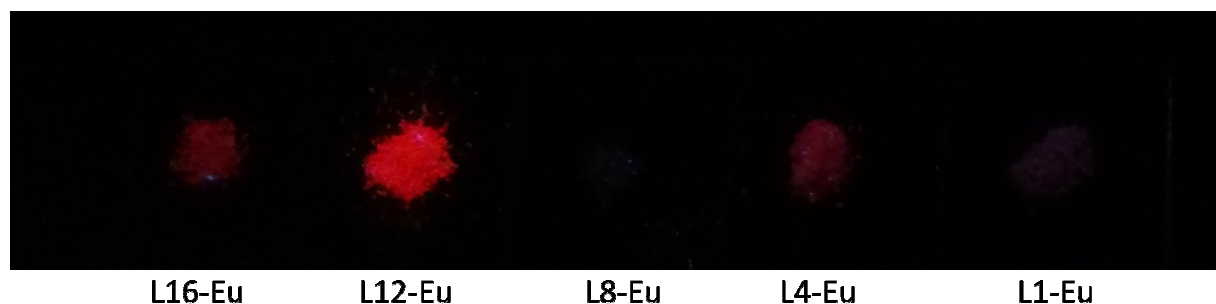L16-Eu   L12-Eu   L8-Eu   L4-Eu   L1-Eu

Fig 4.25 Powdered complexes under UV-light

The self emission was highest in case of L1-Eu and L8-Eu which showed that a significant part of energy was absorbed by ligand itself rather than transferring it to the metal ion. The self emission was lowest in case of L16-Eu and in case of L4-Eu and L12-Eu it was a little higher than L16-Eu. This observation fits well with the triplet state population of ligands. L1 and L8 being fluorescent only did not have high population in triplet state because of which the energy transfer to the Europium metal was not significant while in case of L4, L12 and L16 the energy transfer was much better as compared to L1 and L8 as they were phosphorescence in powdered state (as shown in bar diagram in figure 4.24). Being phosphorescent, they had higher population in triplet

state therefore making a better picture for energy transfer to metal ion. To confirm the trend, solid sample of each complex was kept on quartz plates and were illuminated under UV light. By naked eye it was detected that L4-Eu, L12-Eu and L16-Eu had a much better share of metal emission as compared to the self emission of ligand (fig 4.25). The lifetime study of each europium complex was also done using the pulsed Tungsten lamp by exciting at 330 nm and collecting at 615 nm. The decay profile is shown in figure 4.26. Complexes L1-Eu, L8-Eu, L12-Eu and L16-Eu were fitted mono exponentially while complex L4-Eu was fitted bi exponentially. The lifetime of the complexes was obtained in the range of milliseconds which is characteristics of Europium complexes. The value of lifetime of each complex is given in table 4.4

Complex	T1(ms)	T2(ms)
L16-Eu	0.52	-
L12-Eu	0.44	-
L8-Eu	0.16	-
L4-Eu	0.16	0.71
L1-Eu	0.28	-

Table 4.4: Lifetime value of the complexes
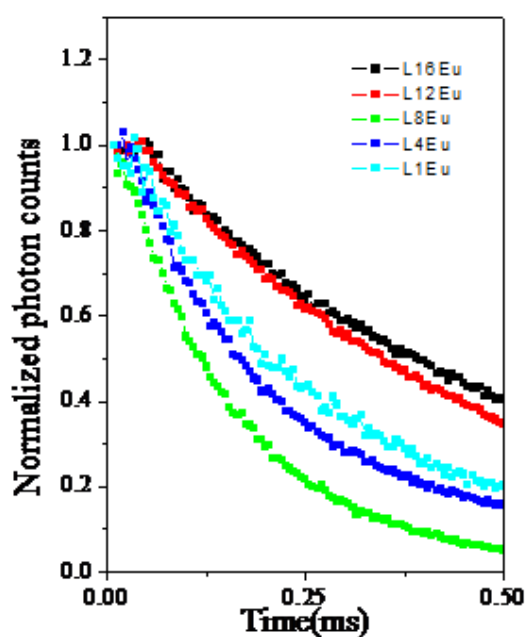
As seen from the decay profile of complexes the decay rate of L12-Eu and L16-Eu was significantly slower as compared to the decay profile of the complexes L1-Eu, L4-Eu and L8-Eu which signifies the long lived triplet state species in L12 and L16 Eu complexes.

Fig 4.26 TCSPS decay profile of Eu complexes

5. CONCLUSION

In this thesis we solved one problem of designing a polymer probe as triple action sensor and this work is the first example to demonstrate the concept of multitasking molecular probe for sensing applications. The custom designed distilbene polymer chromophore is very unique for sensing temperature, metal-ions and biomolecules. Temperature probe was achieved through the polymer ability to act as photosensitizer for Eu^{3+} ions (LMET process) and the turn- Off and turn-On behaviors of red-fluorescence in heating and cooling cycles. Selective metal-ion probe was accomplished for Cu^{2+} ions through the quenching of polymer blue-fluorescence (turn-Off process). Biomolecular probe was achieved by reversibly turn-On the copper-switch in water. The present investigation opens up sensing concept based on single polymer probe for temperature, toxic metal ions and amino acids.

But this polymer needed a coligand to sensitize Europium metal ion and then it acted as temperature sensor. But the presence of coligand makes it difficult for such probes to process and make devices. Therefore in another scheme we addressed this problem by designing five different ligands that can sensitize Europium to different extents in absence of a coligand through triplet state population generation because of heavy atom effect. The ligands and complexes being phosphorescent can be great asset in OLED, biosensing and temperature sensing research because of the ease by which they can be processed.


Future Prospects:

After optimizing the conditions for ligand these ligands can be polymerized by different means and iodine can act as a heavy atom to enhance intersystem crossing making the polymers phosphorescent and the modified polymer can do the same work of triple action sensor as that of PTEG and PHEG but in the absence of a coligand. This will make these systems easy to process and can be devised into an instrument easily making science serve the society.

6. REFERENCES

1. Binnemans, K. *Chem. Rev*. **2009**, *102*, 4283-4374.

2. Eliseeva, S. V.; Bunzli, J. C. G, *Chem. Soc. Rev.* **2010**, *39*, 189-227.

3. Latva, M.; Takalo, H.; Mukkala, V. M.; Matachescu, C.; Rodriguez-Ubis, J. C.; Kanakare, J. , *J. Lumin.* **1997**, *75*, 149-1691.

4.(a)A. Balamurugan, M. L. P. Reddy, and M. Jayakannan, *J. Phys. Chem. B,* **2011**, 115, 10789-10800.(b) A. Balamurugan, M. L. P. Reddy and M. Jayakannan, *J. Phys. Chem. B,* **2009**,*113*, 14128-14138.(c) A. Balamurugan, M. L. P. Reddy and M. Jayakannan*, J. Mater. Chem. A*, **2013**, 1, 2256–2266.

5. Liu, D.; Wang, Z.; Yu, H.; You, J. , *Eur. Polym. J.* **2009**, *45*, 2260-2268.

6. Liu, Y.; Wang, Y.; Guo, H.; Zhu, M.; Li, C.; Peng, J.; Zhu, W.; Cao Y, *J. Phys. Chem. C*, **2011**, *115* , 4209-4216.

7. Forster, S.; Antonietti, M. , *Adv. Mater*. **1998**, *10*, 195-261.

8. Leonov, A. P.; Zheng, J.; Clogston, J. D.; Stern, S. T.; Patri, A. K.; Wei, A., *ACS Nano* **2008**, 2, 2481.

9. Ding, H.; Yong, K.-T.; Roy, I.; Pudavar, H. E.; Law, W. C.; Bergey, E. J.; Prasad, P. N. , *J. Phys. Chem. C* **2007**, 111, 12552.

10. Balamurugan, A.; Kumar, A. G., Boomishankar, R.; Reddy, M. L. P.; Jayakannan, M. *, Chem Plus Chem*, **2013**, 78, 737.

11. Kohler, A., Wilson, J. S. & Friend, R. H. *, Adv. Mater.*, **2002** 14, 701–707.

12. B. Chen, L. Wang, Y. Xiao, F. R. Fronczek, M. Xue, Y. Cui, G. Qian*, Angew. Chem.* **2009**, 121, 508; *Angew. Chem. Int. Ed*. **2009**, 48, 500.

13. Baldo, M. A. et al., *Nature*, **1998**, 395, 151–154 .

14. Wong, W.-Y. & Ho, C.-L *J. Mater. Chem.* , **2009** , 19, 4437–4640.

15. Kearns, D. R. & Case, W. A. , *JACS*,**1966**, 88, 5087–5097.

16. O. Bolton, K. Lee, H.J. Kim, K.Lin, J. Kim, *Nat. Chem.*,**2013**, 3, 205-210.

17. Turro, N. J. Modern Molecular Photochemistry 125–126 ,*University Science Books*, **1991**)

18. Hassel, O. Structural aspects of interatomic charge-transfer bonding*, Nobel Lecture*, 9 June **1970**

19. J. C. Ribierre, A. Ruseckas, K. Knights, S. V. Staton, N. Cumpstey, P. L. Burn, D. W. Samuel, *PRL*, **2008**, 100, 017402.

20. Dongwook Lee,Onas Bolton, Byoung Choul Kim, Ji Ho Youk, Shuichi Takayama, Jinsang Kim, *JACS*, **2013**, 135, 6325-6329

21. B. W. D'andrade and S. R. Forrest, *Adv. Mater.*, **2004**, 16,1585–1595.

22. F. So, J. Kido and P. Burrows, *MRS Bull.*, **2008**, 33, 663–669.**23**. OLED Display Fundamentals and Applications-Takatoshi Tsujimura, John Wiley and sons.

24. S. P. McGlynn, T. Azumi, M. Kinoshita, Molecular Spectroscopy of the Triplet State, Prentice-Hall, Eaglewood Cliff, **1969**.

25. N. J. Turro, Modern Molecular Photochemistry, Benjamin Inc., Menlo Park, **1978**.

26. M. Klessinger, J. Michl, Excited States and Photochemistry of Organic Molecules,VCH, New York**, 1995.**

27. (a**)** S. V. Eliseeva, J. C. G. Bunzli**,** *Chem. Soc. Rev***. 2010,** 39, 189 **(b)** G. Accorsi, A. Listorti, K. Yoosaf, N. Armaroli, *Chem. Soc. Rev***. 2009,** 38, 1690**.**

28. (a) S. M. Borisov, O. S. Wolfbeis, *Anal. Chem. 2006***,** 78**,** 5094 (b) M. Mitsuishi, S. Kikuchi, T. Miyashita, Y. Amao, *J. Mater. Chem*. **2003**, 13, 2875.

29. (a) M. Formica,V. Fusi, L. Giorgi, M. Micheloni. *Coord. Chem. Rev.* **2012**, 256, 170 (b) C. Xing, M. Yu, S. Wang, Z. Shi, Y. Li, D. Zhu, *Macromol. Rapid Commun.* **2007**, *28*, 241.

30. J. R. Lakowicz *Principles of Fluorescence Spectroscopy*; Plenum Press: New York, **1983.**

31. A. S. Castillo, M. C. Robles, R. Mallavia, *Chem. Commun*, **2010**, 46, 1263.

32.Z. Guo, W. Zhu, H. Tian *Macromolecules*, **2010**, 43, 739.
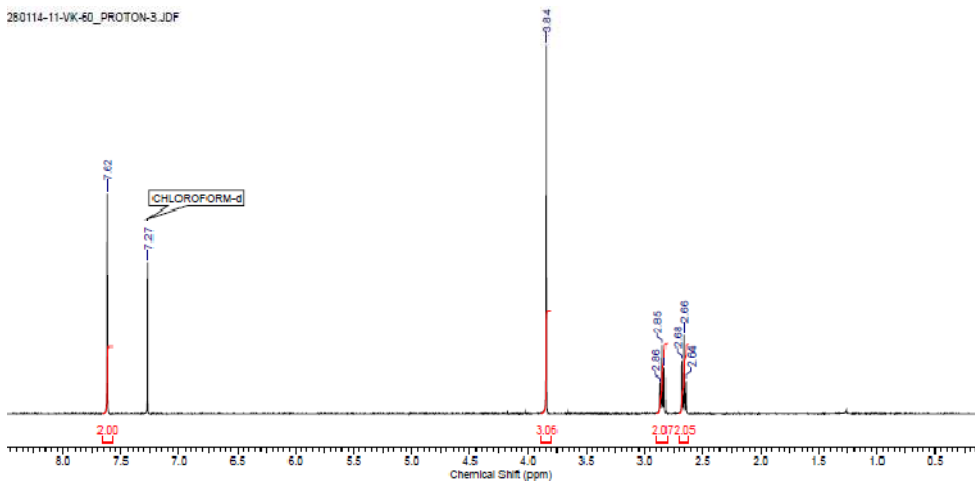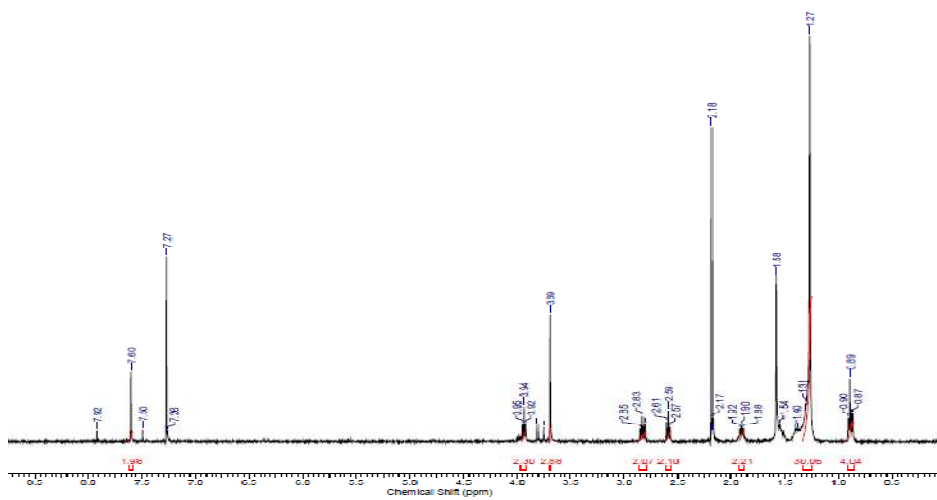
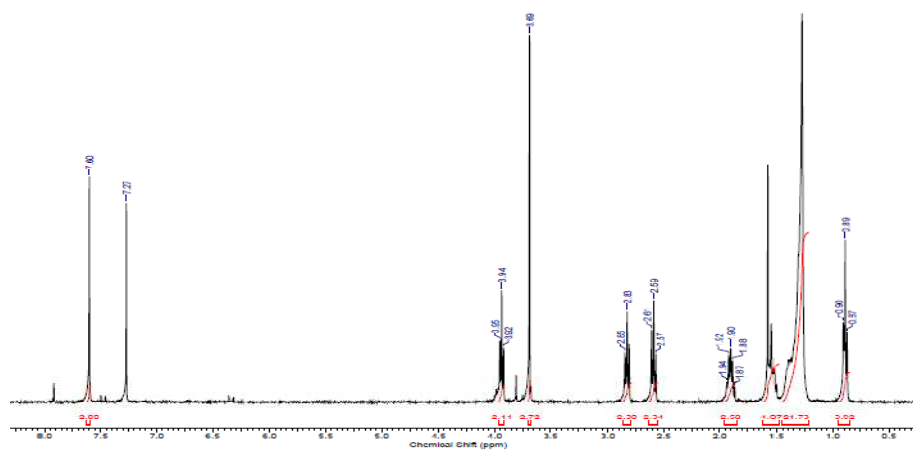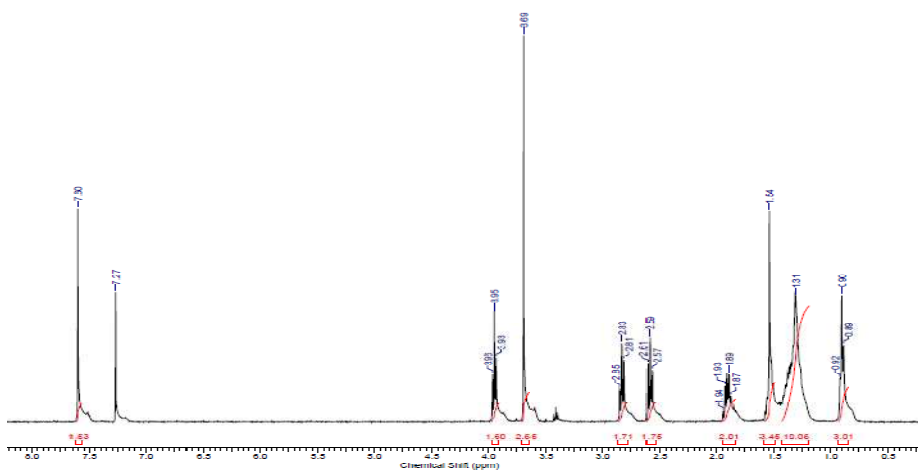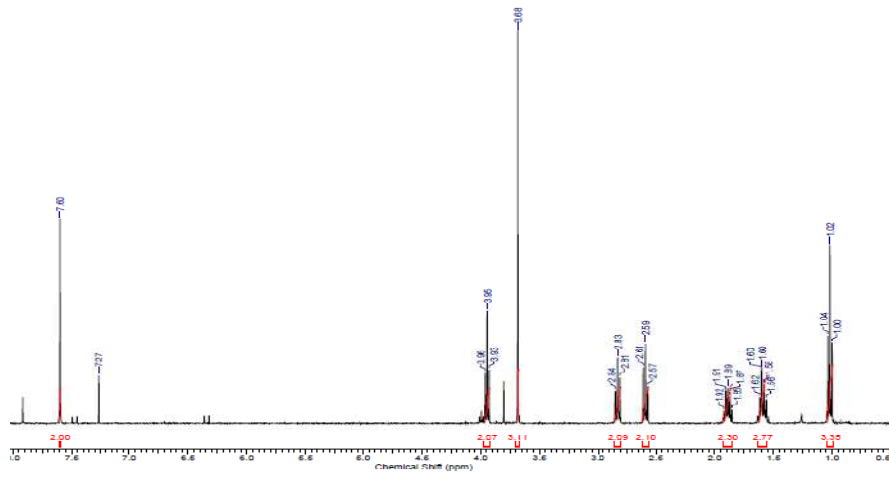# 7. APPENDIX
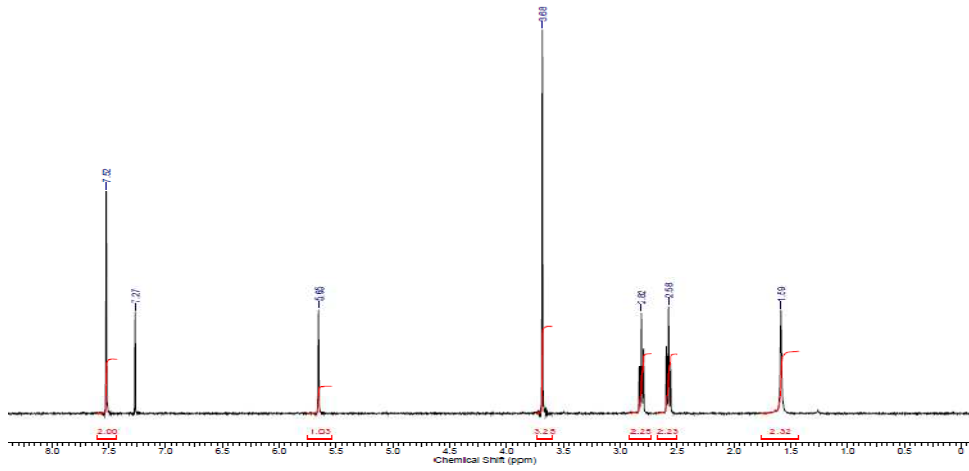
1H NMR of 2
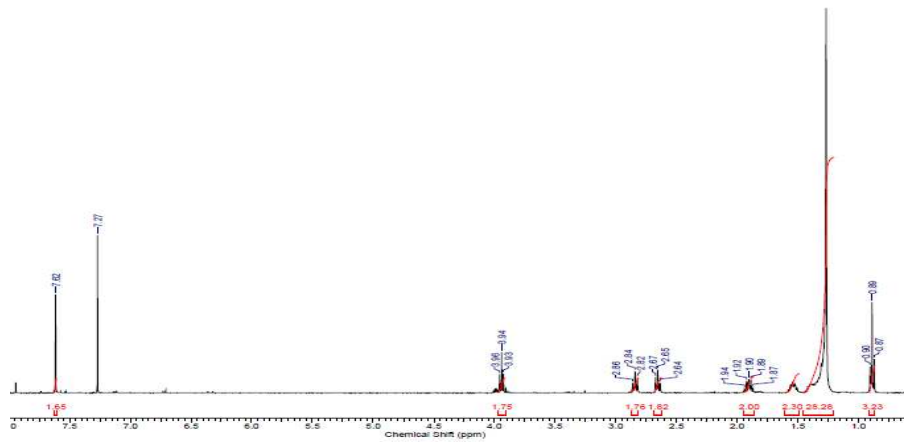

1H NMR of 3

1H NMR of L1
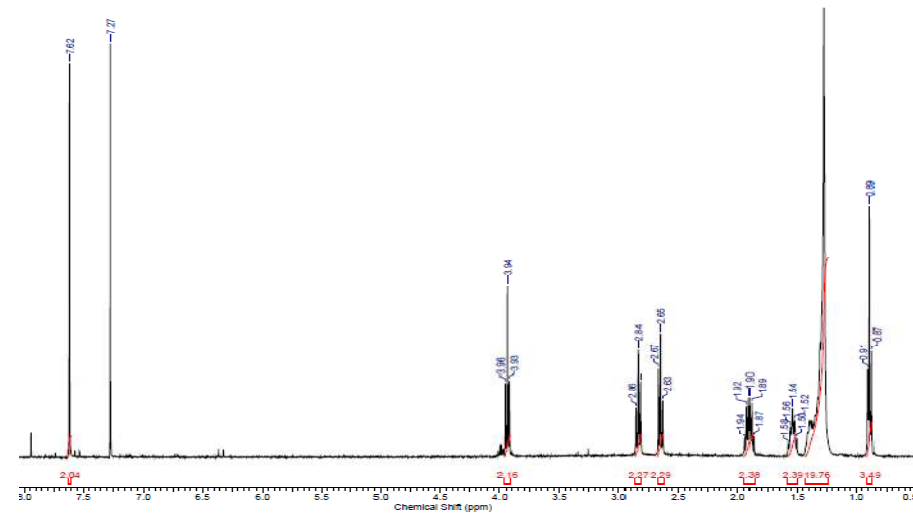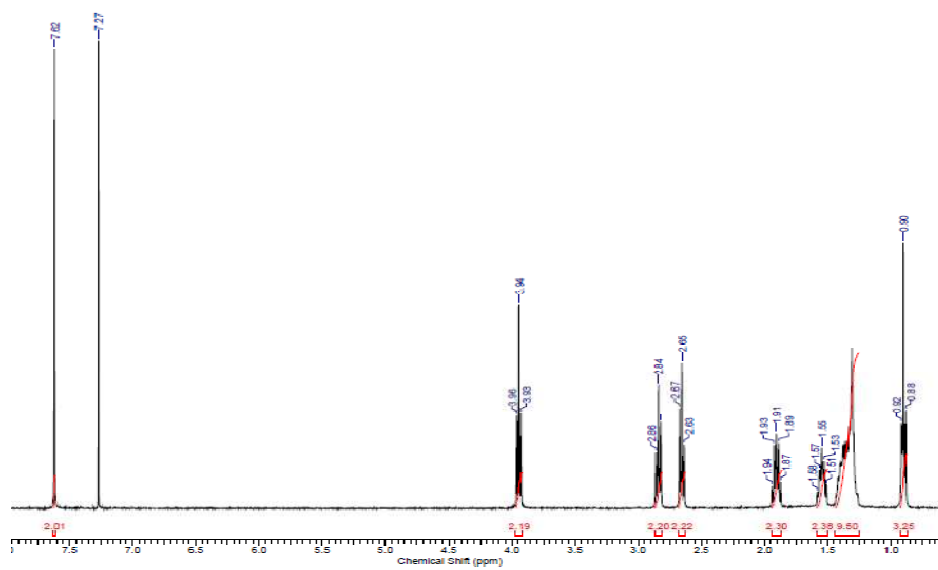
54
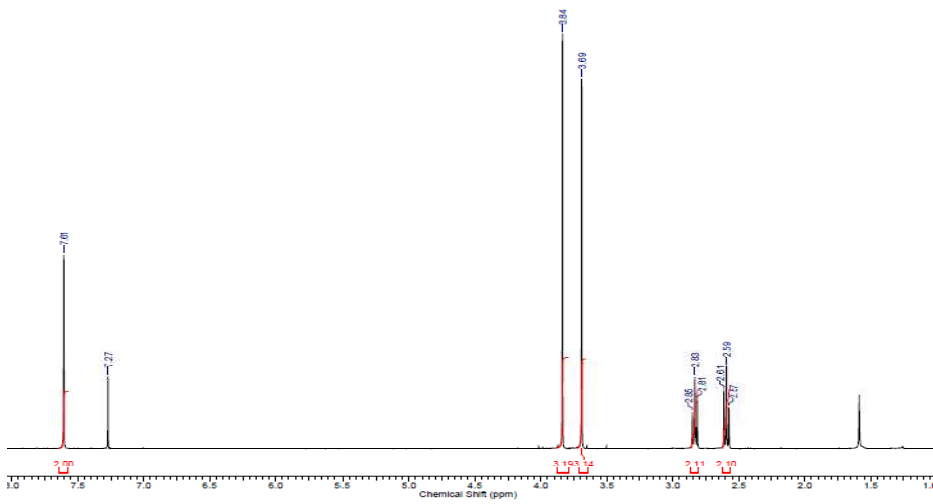
1H NMR of 4a

1HNMR of 4b

1H NMR of 4c

1H NMR of 4d

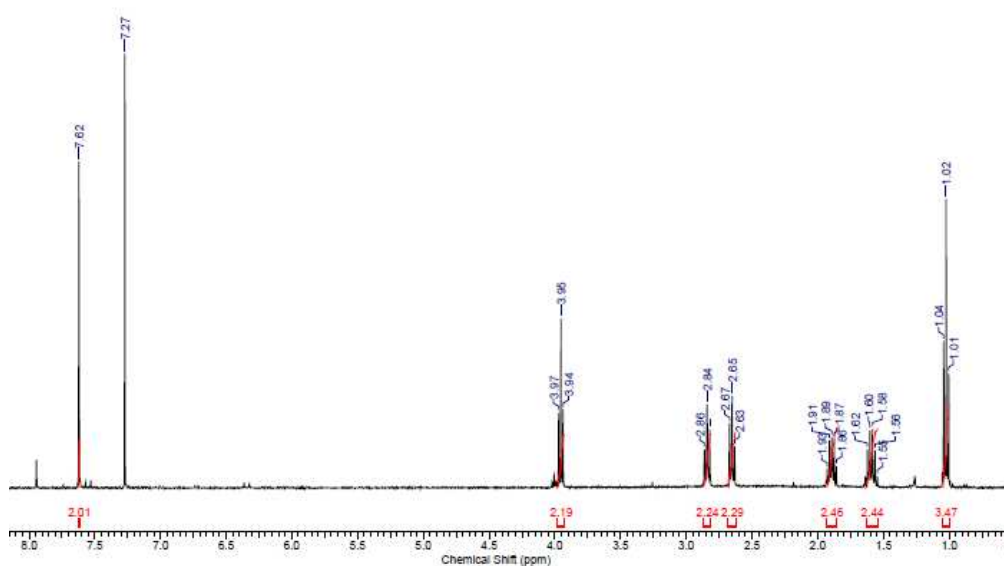1H NMR of L16

1H NMR of L12

56

1H NMR of L8

1H NMR of L4

ChemComm

Triple action polymer probe: carboxylic distilbene fluorescent polymer chemosensor for temperature, metal-ions and biomolecules†

A. Balamurugan, Vikash Kumar and M. Jayakannan*

A triple-action π-conjugated polymer chemosensor is developed for sensing temperature, selective detection of copper(II) metal-ion and biological species – amino acids, in two wavelength optical switches based on red-fluorescent and blue-fluorescent molecular probes.

Single molecular probes for the detection of multiple species or stimuli is one of the most important tasks yet to be achieved in chemical and biological sensing. Dual sensing fluorescent probes have been reported for the ratiometric detection of different metal ions;[1] different anions[2] or metal-ions along with proteins and sugars.[3] However, there is no report up to now for triple-action molecular probes based on either small molecules or polymers. Thus, designing new triple or multiple-action molecular probes is important for fundamental understanding as well as developing new tools for sensing more than two different species or processes. The above problem is addressed based on a distilbene fluorescent polymer probe having unique photosensitizing ability to produce red and blue luminescent readouts.

Here we report a triple-action fluorescent polymer probe for sensing temperature, exclusive detection of toxic metal-ions such as copper(II) and amino acids (Fig. 1). For this purpose, new water-soluble carboxylic functionalized distilbene chromophore bearing polymers were designed and developed. The newly developed polymer has unique ability to function as a triple probe *via* three independent processes: (i) red fluorescent temperature switch *via* ligand to metal energy transfer (LMET) from the polymer to Eu^{3+} ions, (ii) blue fluorescent metal-ion switch by heavy-atom effect with exclusive selectivity for Cu^{2+} ions and (iii) as a biomolecule switch (for amino acids).

Two segmented polymers PTEG and PHEG were synthesized having identical distilbene chromophores with triethylene glycol (TEG) and hexaethylene glycol (HEG) units as spacers in the main chain (Fig. 1). The carboxylic functionalized distilbene chromophore
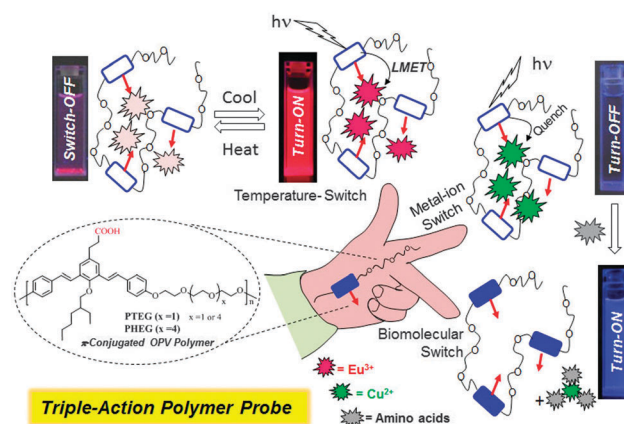
*Department of Chemistry, Indian Institute of Science Education and Research, Dr Homi Bhabha Road, Pune, Maharashtra-411008, India.
E-mail: jayakannan@iiserpune.ac.in; Web: http://www.iiserpune.ac.in/~jayakannan/;
Fax: +91-20-2589 8022*
† Electronic supplementary information (ESI) available. See DOI: 10.1039/c3cc45274c

Fig. 1 Triple-action distilbene chromophore bearing polymer as temperature, metal-ion and biomolecular fluorescent probes.

design was adopted based on our previous experience with π-conjugated polymer photosensitizers.[4] Earlier investigation on the above polymer design revealed that carboxylic functionalized distilbene polymer design was very crucial for achieving temperature sensing in polymer–Eu^{3+} complex in both solution and solid state.[5] Phenylpropionic acid was used as starting material and polymers were made through multi-step synthesis (Fig. SF-1†).‡ The characterizations of these polymers are given in the ESI† (Fig. SF-2 and SF-3). The molecular weight of the polymers were obtained as M_n = 8000–8300 and M_w = 16 000–24 000. The carboxylic acid groups were converted into their sodium salts for sensing. The absorbance and emission spectra of the polymers exhibited maxima at 310 and 410 nm, respectively (Fig. SF-4†). The polymers were subjected for absorbance and emission studies at various pH. The plots of photoluminescence intensity *vs.* pH showed a non-linear trend with a break point near pH = 6.0–7.0 (Fig. SF-5–SF-7†). This revealed that at lower pH (in acidic medium) the chain interaction quenched the chromophore fluorescence. At higher pH, the negatively charged carboxylate anion in the distilbene chromophore caused separation of the chains, leading to enhancement in emission. At neutral pH, the polymers exhibited the optimum conformation
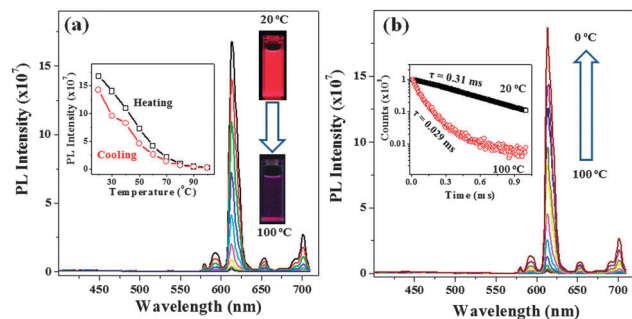
Fig. 2 Temperature probe of PHEG–Eu^{3+} complex at 1.8×10^{-6} M (repeat unit concentration) in the heating (a) and cooling (b) cycles (in chlorobenzene). The inset in (a) showed the plots of PL intensity at various temperatures (λ_{ex} = 350 nm). The inset in (b) showed the TCSPC profiles of polymer–Eu^{3+} at 20 and 100 °C.

for sensing studies (Fig. SF-7†). The fluorescence quantum yields of polymers were determined at pH = 7.4 as 0.08 and 0.11 for PTEG and PHEG, respectively, using quinine sulfate as standard (ϕ = 0.53 in 0.1 N H$_2$SO$_4$).

A temperature sensing probe was developed using the polymer PHEG (also PTEG) in complexation with Eu^{3+} ions.[5] The polymers were found to be selective photosensitizers to Eu^{3+} ions compared to other lanthanides. The polymer ligand to metal-ion excitation energy transfer (LMET) showed characteristic Eu^{3+} strong metal centered sharp emission (λ_{ex} = 350 nm) peaks at 580, 593, 614, 650 and 702 nm corresponding to various D → F transitions[5,6] (Fig. 2a at 20 °C). The photograph of the polymer–Eu^{3+} complex (in Fig. 2) showed strong red emission in solution confirming complete excitation energy transfer from the blue-emitting π-conjugated distilbene polymer backbone. The occurrence of LMET process in the complexes was validated from their singlet and triplet energies of the polymeric ligands and the excited energy levels of Eu^{3+} ions (for details, Fig. SF-8†).

The polymer–Eu^{3+} ion complex showed unique temperature sensing in chlorobenzene, THF, DMSO and p-xylene. The strong and sharp red emission at 20 °C was gradually diminished while heating up to 100 °C (Fig. 2a, in chlorobenzene). In the subsequent cooling cycle, the red emission recovered completely while cooling from 100 to 20 °C (Fig. 2b). The FL-intensities of the red-emission at 615 nm were plotted against the temperature and shown as an inset in Fig. 2a. The temperature turn-on and turn-off switch was found to work at 72 °C (shown by arrow) (55 °C for TEG complex, Fig. SF-9†). The temperature sensing ability of the PHEG–Eu^{3+} ion complex arose by the destabilization of Eu^{3+} ion excited state (^{5}D$_0$ states) at higher temperatures[7] (Fig. SF-8† for more detail). The recovery of fluorescence from Eu^{3+} ion showed hysteresis and the original value was recovered only at 0 °C. TCSPC profiles for PHEG–Eu^{3+} are given as inset in Fig. 2b (λ_{ex} = 350 nm and collected at 612 nm). The lifetime of the excited species were found to be 3.1 ms at 20 °C whereas it drastically decreased to 21 μs at 100 °C. The decay profiles were also found to be completely reversible in the subsequent cooling cycles. Thus, the thermosensitive probe of polymer–Eu^{3+} ions complexes worked by two processes: (i) turn-on via LMET from the polymer to Eu^{3+} ions and (ii) turn-off through the destabilization of ^{5}D$_0$ excited states of the metal-centre.

The metal-ion sensing of the polymer probe was performed in PIPES buffer at pH 7.4. The absorption spectra of the polymers showed 8–10 nm blue shift with increase in the concentrations of Cu^{2+} ion (Fig. SF-10†). Upon addition of metal ions into the sodium salt of the polymers, the metal complex formed with carboxylate anion by displacing the sodium ion. This indicated the formation of polymer–Cu^{2+} ion complexes. The fluorescence responses of the PHEG–Na$^+$ polymer at various Cu^{2+} ion concentrations are shown in Fig. 3a. The polymer emission was found to quench drastically with increase in Cu^{2+} ion concentration. The polymer showed complete quenching (more than 97%) at 24 μM of Cu^{2+} ion indicating their upper detection limit. The fluorescence turn-off switch in these π-conjugated systems towards Cu^{2+} ion was attributed to the quenching of excitation energy by the metal-ions through heavy atom effect.[8] The lower detection limits of both PTEG and PHEG polymers for Cu^{2+} metal ion were 3 μM. To further quantify the turn-off efficiencies of these polymers, the fluorescence intensity of the polymers at Cu^{2+} ion at various concentrations were fitted to the Stern–Volmer equation: $I_0/I = 1 + K_{sv}[\text{Cu}^{2+}]$, where I_0 and I are the initial and final emission intensity of the chromophores and K_{sv} is the Stern–Volmer quenching constant.[9] The inset Fig. 3a, showed the Stern–Volmer plots of polymers for Cu^{2+} ion. The plots exhibited a typical non-linear trend with respect to both static and dynamic fluorescence quenching towards the analytes. The Stern–Volmer constants were obtained as 6.1×10^5 M^{-1} and 4.5×10^5 M^{-1} for PTEG and PHEG polymers, respectively. The K_{sv} values from the polymer probes are comparable to that of other probes reported for Cu^{2+} ion sensing.[10,11]

The selectivity of the polymer probes towards Cu^{2+} ions over other metal cations were also tested (Fig. 3b). The fluorescence quenching experiments were carried out for more than 12 metal cations from alkali and transition groups: Na$^+$, K$^+$, Li$^+$, Ca^{2+}, Mg^{2+}, Pb^{2+}, Ag$^+$, Zn^{2+}, Hg^{2+} and Co^{2+} ions in PIPES buffer solutions at pH 7.4. The fluorescence quenching ability of each of these metal ions at various concentrations are given in Fig. SF-11–SF-16 (ESI†). The fluorescence responses of the polymers at 24 μM Cu^{2+} concentration are shown in Fig. 3b. The bar diagram (Fig. 3b) evidences that most of these metal
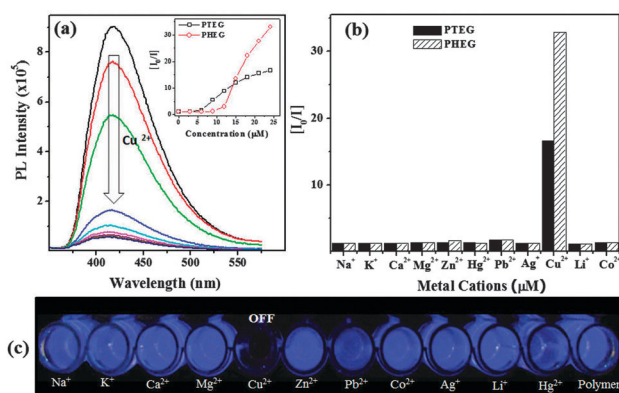

Fig. 3 (a) Emission spectra of PHEG–Na$^+$ in 5×10^{-6} M (repeat unit concentration) in PIPES buffer with the concentration of Cu^{2+} ions varied from 3 μM to 24 μM in PIPES buffer (λ_{ex} = 310 nm). The inset in (a) showed the plots of I_0/I variation over the concentration of Cu^{2+} ions. (b) I_0/I values for various metal ions at 24 μM in PIPES buffer. (c) Photographs of vials.

ions showed very little to negligible sensing comparable to the super-quenching observed in Cu^{2+} ion. It is clear in Fig. 3b that fluorescence quenching efficiency of polymers by Cu^{2+} ions is nearly 20–30 times higher compared to other metal ions. The selectivity of the polymer towards the Cu^{2+} ion can be clearly seen in the photograph shown in Fig. 3c. These results suggest that both PTEG and PHEG have good selectivity towards Cu^{2+} ion even in the presence of other alkali, alkaline, heavy and transition-metal ions. Further, the polymer probes did not show any interference with other divalent transition metals (Pb(II) or Hg(II) ions)[12] and showed high selectivity towards Cu^{2+} ions in water. The sensing ability of the polymer probe also showed remarkable difference with respect to the number of oligoethyleneoxy units in the backbone. The effect of hexaethyleneoxy spacer polymer (PHEG) was found to be almost twice compared to triethyleneoxy chain counterparts (PTEG) (data in Fig. 3b). This difference is attributed to the ability of the distilbene chromophores in polymer backbone to scavenge the metal ions. Longer segmented spacers provide more degree of flexibility for the distilbene chromophores to wrap around the Cu^{2+} ion which is relatively less preferred in the shorter segments.

Biomolecule probing was tested based on the turn-on ability of the quenched polymer–Cu^{2+} by biological molecules. This turn-on switch was investigated for anions such as phosphates and variety of L-amino acids.[13,14] Amino acids disrupt the polymer–Cu^{2+} complex (turn-off switch) in aqueous medium by strongly complexing with Cu^{2+} ions compared to carboxylate distilbene chromophores in the polymer backbone. The completely fluorescence quenched polymer (95%) solutions containing 24 μM of Cu^{2+} in PIPES buffer (at pH = 7.4) was chosen for sensing amino acids.

Six different amino acids were chosen for the sensing studies: alanine, serine, cysteine, glutamine, histidine and tryptophan. These amino acids have diverse functional groups such as $-NH_2$, $-OH$, $-COOH$, $-SH$, $-CONH_2$, imidazole and indole; thus their complexation with Cu(II) ions may vary significantly in sensing studies. The fluorescence responses of the polymers were monitored by varying the concentration of amino acids and phosphates (details provided in Fig. SF-17–SF-21†). The fluorescence response with respect to the addition of the amino acid histidine is shown in Fig. 4a. In the present system, only 25% of fluorescence was recovered which may be due to incomplete formation Cu(II)–amino acid complex. Further, the detection capabilities of these amino acids are also checked at various concentrations from 5 to 50 μm (Fig. SF-21†). At 30 μm concentration, almost all the amino acids attained the maximum sensing ability (Fig. SF-21†). The bar diagram in Fig. 4b clearly shows the recovery of fluorescence intensity for histidine which is at least 2–3 times higher compared to other amino acids. The sensing by tryptophan and glutamine were second best compared to histidine. Alanine, cysteine and serine showed relatively weak sensing capabilities. This revealed that heterocyclic ring in histidine binds more strongly to Cu(II) ions compared to other functional groups in amino acids. Among all the amino acids, cysteine attained the saturation level quickly at 5 μm concentration whereas other amino acids reached the maxima at higher concentration (24–30 μm, Fig. SF-21†). This trend was attributed to the thiophilic nature of cysteine towards Cu(II). In order to check the selectivity of histidine over other amino acids and also to study the effect of temperature on
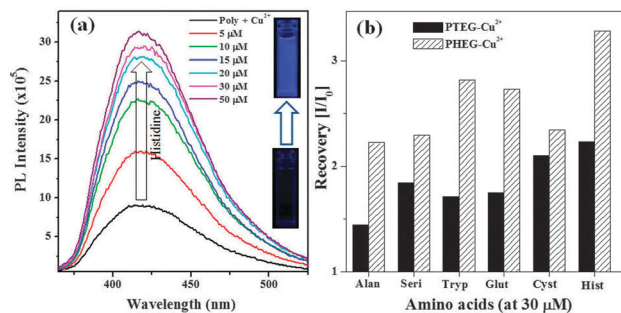

Fig. 4 (a) Fluorescence response from the PHEG–Cu^{2+} ion complex (using 5×10^{-6} M of PHEG–Na^+ + 24 μM Cu^{2+} ion) upon the addition of 5–50 μM histidine in PIPES buffer (λ_{ex} = 310 nm). (b) I/I_0 values for various amino acids at 30 μM.

the sensing studies; sensing experiments were carried out for histidine with cysteine and alanine at two different temperatures, 25 and 60 °C (Fig. SF-22 and SF-25†). PHEG–Cu^{2+} quenched probe (with 30 μM Cu^{2+} ions) was treated with 30 μM histidine followed by 30 μM alanine or cysteine and vice versa. At 25 °C, the recovery of the fluorescence switch was observed as 45% for the addition of histidine into alanine whereas the reverse addition showed only 14% enhancement (Fig. SF-22†). At 60 °C, the performance of the switch was found to be relatively poor with only 23% recovery for the addition of histidine after alanine (Fig. SF-23†). A similar experiment for cysteine and histidine combination at 25 and 60 °C (Fig. SF-24 and SF-25†) revealed that the thio-group in cysteine strongly interferes with selectivity of histidine. Thus, it may be concluded that simple amino acids such as alanine did not interference with histidine selectivity. Further ambient temperature was found to be suitable for biomolecule sensing.

The present work is the first example to demonstrate the concept of triple-action molecular probe for sensing applications. The custom designed distilbene polymer chromophore is unique for sensing temperature, metal-ions and biomolecules. Temperature probe was achieved through the polymer ability to act as a photosensitizer for Eu^{3+} ions (LMET process) and the turn-off and turn-on behaviors of red-fluorescence in heating and cooling cycles. Selective metal-ion probe was accomplished for Cu^{2+} ions through the quenching of polymer blue-fluorescence (turn-off process). Biomolecular probe was achieved by reversible turn-on of the copper-switch in water. The present investigation opens up sensing concept based on single polymer probe for temperature, toxic metal ions and amino acids.

Notes and references

‡ The synthesis of polymers, structural characterization, details on the sensing procedures, additional emission and absorbance spectra of temperature sensing, metal-ion sensing and biomolecule sensing are given in the ESI.†

1 (a) H. N. Kim, W. X. Ren, J. S. Kim and J. Yoon, Chem. Soc. Rev., 2012, 41, 3210; (b) E. M. Nolan and S. J. Lippard, Chem. Rev., 2008, 108, 3443.

2 (a) S. Sreejith, P. Carol, K. P. Divya and A. Ajayaghosh, *J. Mater. Chem.*, 2008, **18**, 264; (b) Z. Xu, X. Chen, H. N. Kim and J. Yoon, *Chem. Soc. Rev.*, 2010, **39**, 127.

3 (a) Y. Zhou and J. Yoon, *Chem. Soc. Rev.*, 2012, **41**, 52; (b) J. Hou, F. Song, L. Wang, G. Wei, Y. Cheng and C. Zhu, *Macromolecules*, 2012, **45**, 7835.

4 (a) A. Balamurugan, M. L. P. Reddy and M. Jayakannan, *J. Phys. Chem. B*, 2009, **113**, 14128; (b) A. Balamurugan, M. L. P. Reddy and M. Jayakannan, *J. Phys. Chem. B*, 2011, **115**, 10789; (c) A. Balamurugan, M. L. P. Reddy and M. Jayakannan, *J. Polym. Sci., Part A: Polym. Chem.*, 2009, **47**, 5144.

5 A. Balamurugan, M. L. P. Reddy and M. Jayakannan, *J. Mater. Chem. A*, 2013, **1**, 2256.

6 (a) S. V. Eliseeva and J. C. G. Bunzli, *Chem. Soc. Rev.*, 2010, **39**, 189; (b) G. Accorsi, A. Listorti, K. Yoosaf and N. Armaroli, *Chem. Soc. Rev.*, 2009, **38**, 1690.

7 (a) S. M. Borisov and O. S. Wolfbeis, *Anal. Chem.*, 2006, **78**, 5094; (b) M. Mitsuishi, S. Kikuchi, T. Miyashita and Y. Amao, *J. Mater. Chem.*, 2003, **13**, 2875.

8 (a) M. Formica, V. Fusi, L. Giorgi and M. Micheloni, *Coord. Chem. Rev.*, 2012, **256**, 170; (b) C. Xing, M. Yu, S. Wang, Z. Shi, Y. Li and D. Zhu, *Macromol. Rapid Commun.*, 2007, **28**, 241.

9 J. R. Lakowicz, *Principles of Fluorescence Spectroscopy*, Plenum Press, New York, 1983.

10 A. S. Castillo, M. C. Robles and R. Mallavia, *Chem. Commun.*, 2010, **46**, 1263.

11 Z. Guo, W. Zhu and H. Tian, *Macromolecules*, 2010, **43**, 739.

12 I. B. Kim, B. Erdogan, J. N. Wilson and U. H. F. Bunz, *Chem.–Eur. J.*, 2004, **10**, 6247.

13 X. Zhao, Y. Liu and K. S. Schanze, *Chem. Commun.*, 2007, 2914.

14 Y. Bao, H. Wang, Q. Li, B. Liu, Q. Li, W. Bai, B. Jin and R. Bai, *Macromolecules*, 2012, **45**, 3394.